chemistry

MDPI

Article

Bioactive Pyrrolo[2,1-*f*][1,2,4]triazines: Synthesis, Molecular Docking, In Vitro Cytotoxicity Assay and Antiviral Studies

Nataliya N. Mochulskaya [1], Svetlana K. Kotovskaya [1], Ilya I. Butorin [1], Mikhail V. Varaksin [1,*], Valery N. Charushin [1], Vladimir L. Rusinov [1], Yana L. Esaulkova [2], Alexander V. Slita [2], Polina A. Ilyina [2] and Vladimir V. Zarubaev [2]

[1] Department of Organic and Biomolecular Chemistry, Ural Federal University Named after the First President of Russia B.N. Yeltsin, Mira Street, 19, Yekaterinburg 620002, Russia; n.n.mochulskaia@urfu.ru (N.N.M.)
[2] Saint-Petersburg Pasteur Institute, Mira Street, 14, Saint Petersburg 197101, Russia
* Correspondence: m.v.varaksin@urfu.ru

Abstract: A series of 2,4-disubstituted pyrrolo[2,1-*f*][1,2,4]triazines containing both aryl and thienyl substituents were synthesized by exploiting the 1,3-cycloaddition reaction of N(1)-ethyl-1,2,4-triazinium tetrafluoroborates with dimethyl acetylenedicarboxylate. The antiviral activity of the synthesized compounds against influenza virus strain A/Puerto Rico/8/34 (H1N1) was studied in experiments on Madin-Darby canine kidney (MDCK) cell culture. Among the pyrrolo[2,1-*f*][1,2,4]triazine derivatives, compounds with low toxicity and high antiviral activity were identified. Dimethyl 4-(4-methoxyphenyl)-7-methyl-2-*p*-tolylpyrrolo[2,1-*f*][1,2,4]triazine-5,6-dicarboxylate was found to demonstrate the best antiviral activity (IC_{50} 4 μg/mL and selectivity index 188). Based on the results of in vitro tests and molecular docking studies performed, a plausible mechanism of action for these compounds was suggested to involve inhibition of neuraminidase.

Keywords: 3,5-disubstituted 1,2,4-triazines; 1,3-dipolar cycloaddition; 2,4-disubstituted pyrrolo [1,2,4]triazines; influenza; molecular docking

Citation: Mochulskaya, N.N.; Kotovskaya, S.K.; Butorin, I.I.; Varaksin, M.V.; Charushin, V.N.; Rusinov, V.L.; Esaulkova, Y.L.; Slita, A.V.; Ilyina, P.A.; Zarubaev, V.V. Bioactive Pyrrolo[2,1-*f*][1,2,4] triazines: Synthesis, Molecular Docking, In Vitro Cytotoxicity Assay and Antiviral Studies. *Chemistry* **2023**, *5*, 2657–2676. https://doi.org/10.3390/chemistry5040171

Academic Editors: Maria G. P. M. S. Neves, M. Amparo F. Faustino and Nuno M. M. Moura

Received: 25 September 2023
Revised: 17 November 2023
Accepted: 17 November 2023
Published: 21 November 2023

1. Introduction

Influenza is known to be one of the most widespread infectious diseases worldwide. This infection is caused by influenza virus types A, B and C (the family of Orthomyxoviridae, genus Influenzavirus), has a tendency to epidemically spread and affects all age groups of the population in various geographical conditions. Type A virus is the most common and is the cause of the major pandemics. A large number of cases of severe/complicated influenza, as well as deaths, are recorded annually, which are associated with high morbidity and involvement in the epidemic process of people from risk groups for an unfavorable course of the disease [1,2].

For the treatment and prophylaxis of influenza, the WHO recommends the use of ethiotropic drugs that have a direct effect on the reproduction of the virus. Anti-influenza drugs currently used in clinical practice are aimed at inhibiting the activity of influenza virus proteins: neuraminidase (oseltamivir, zanamivir, laninamivir, peramivir), M2-proton channel (amantadine and rimantadine), PA endonuclease (baloxavir marboxil), RNA-dependent RNA polymerase complex (favipiravir, ribavirin) [3–8]. Modern methods for specific prophylaxis and treatment of influenza are not always effective, because of rapid mutations of the virus and the emergence of drug resistance. Thus, all currently circulating influenza viruses are resistant to the M2-channel blockers, and cases of resistance to baloxavir marboxil, approved for clinical use in 2018, have already been recorded [9–11].

Recent studies have revealed new compounds that target other influenza viral proteins: NP-inhibiting nucleosin [12], inhibitors of the cap-binding activity of PB2 protein [13,14], inhibitors targeting hemagglutinin (HA) [15–18].

The pyrrolo[2,1-*f*][1,2,4]triazine scaffold appears to be a unique heterocyclic system, which is positioned by the scientific community as a multimodal pharmacophore and a privileged structural motif for drug development [19].

Traditionally, pyrrolo[2,1-*f*][1,2,4]triazines, as structural analogues of purine bases, are considered as potential antiviral compounds. Indeed, nucleosides based on pyrrolo[2,1-*f*][1,2,4]triazines demonstrate antiviral activity against various RNA viruses: hepatitis C, Marburg, Ebola, parainfluenza, measles, mumps, human immunodeficiency, respiratory syncytial virus (RSV) and norovirus [20–22].

Pyrrolo[2,1-*f*][1,2,4]triazine derivatives can be regarded as structural analogues of non-nucleoside antiviral drugs, namely riamilovir (Triazavirin®) (Figure 1A). The latter has recently been registered as an antiviral drug and approved for medical treatment of influenza, ARVI and manifestations of tick-borne encephalitis virus fever [23]. The previously studied pyrrolotriazines demonstrate a relatively low cytotoxicity and are characterized by high selectivity indices against influenza virus A/Puerto Rico/8/34 (H1N1) (Figure 1B) [24].

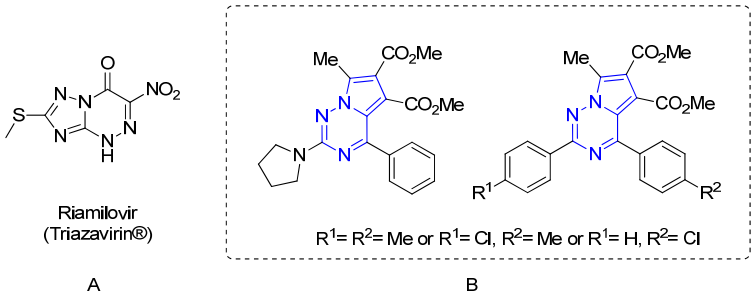

Figure 1. Non-nucleoside antiviral drug Riamilovir (**A**) and pyrrolo[2,1-*f*][1,2,4]triazines (**B**).

Pyrrolo[2,1-*f*][1,2,4]triazines can be regarded as a family of promising therapeutic agents against infectious diseases, hence the development of methods for the synthesis of new compounds of this series merits consideration as an urgent task.

The aim of this study is to elaborate new approaches based on 1,3-dipolar cycloaddition (1,3-DP CA) methodology for the synthesis of 2,4-disubstituted pyrrolo[2,1-*f*][1,2,4]triazines and to evaluate their activity against influenza virus A/Puerto Rico/8/34 (H1N1), followed by assessment of the plausible mechanism of action, by exploiting molecular docking studies on the key influenza proteins.

2. Materials and Methods

2.1. Chemistry

2.1.1. General

Commercial reagents were obtained from Sigma-Aldrich (Darmstadt, Germany), Acros Organics (Geel, Belgium) or Alfa Aesar (Heysham, UK) and used without any further purification. The solvents were purified and dried by standard methods before use.

The progress of reactions was monitored by TLC on Silufol 254 or P-A-UV-254 ("Sorbfil") plates in benzene–ether (15:1) or acetone–hexane (1:4) systems. ^{1}H and ^{13}C NMR spectra were recorded on a Bruker Avance NEW 600, Bruker DRX 400 spectrometers (Bruker AXS GmbH, Karlsruhe, Germany) at 600.13 and 400.13 MHz frequencies for protons, 151 and 101 MHz for carbon. The values of chemical shifts in the ^{1}H and ^{13}C NMR spectra are given relative to the residual signal of protons and carbon atoms of the deuterated solvent.

Chemical shifts are reported in ppm, and coupling constants are given in Hz. Data for ^{1}H NMR are recorded as follows: chemical shift (ppm), multiplicity (s, singlet; d, doublet; t, triplet; q, quartet; quin, quintet; sex, sextet; m, multiplet; br s, broad signal), integration and coupling constant (Hz).

Mass spectra were recorded on a Shimadzu GCMS-QP2010 Ultra instrument (Shimadzu, Kyoto, Japan) (EI-MS). Elemental analyses were performed on a PerkinElmer 2400 elemental analyzer (Perkin Elmer, Waltham, MA, USA). Melting points were determined on a Stuart SMP3 (Bibby Scientific, Stone, UK) and are uncorrected.

Aryl(thiophen-2-yl)amidrazones **1**–**4** were prepared from the corresponding nitriles according to the reported procedure [25]. Aryl(thiophen-2-yl)glyoxals **5a**–**h** and their monohydrates were synthesized by oxidation of the substituted acetophenones, 2-acetylnaphthalene and 2-acetylthiophene with selenium dioxide in dioxane according to the described methods [26,27].

The synthesis of 3,5-disubstituted 1,2,4-triazines **6**–**9** was carried out via cyclization of the corresponding aryl(thiophen-2-yl)amidrazones **1**–**4** with aryl(thiophen-2-yl)glyoxals **5a**–**h** according to the modified procedure [28].

2.1.2. Preparation of 3-R^1-5-R^2-1,2,4-triazines **6**–**9** (General Method)

To a solution (suspension) of aryl(thiophen-2-yl)glyoxal hydrate **5a**–**h** (20 mmol) in ethanol cooled to 0 °C was added in portions a cooled solution of aryl(thiophen-2-yl)amidrazone **1**–**4** (20 mmol) in ethanol so that the temperature of the reaction mixture did not exceed 0–5 °C. The reaction mixture was incubated at +5 °C for 24–48 h, the precipitate was filtered off and recrystallized (see Supplementary Materials Figures S1–S5 for the ^{1}H NMR and mass spectra data of compounds **6e**, **6h**, **7e**, **7f**, **8h**).

3,5-Diphenyl-1,2,4-triazine (**6a**). Yield 55%, yellow powder. Mp 81–83 °C (from propanol-2) (Lit. [29,30] mp 80–84 °C. ^{1}H NMR (400 MHz, DMSO-d_6), δ, ppm (*J*, Hz): 7.62–7.71 (6H, m, Ph); 8.47–8.50 (2H, m, Ph); 8.57–8.60 (2H, m, Ph); 10.06 (1H, s, H-6). EI-MS (70 eV), *m/z* (Irel (%)): 233 $[M]^{+\cdot}$ (5), 103 (13), 103 (9), 102 (100), 76 (11). Found, %: C 77.20; H 4.80; N 18.23. $C_{15}H_{11}N_3$. Calculated, %: C 77.23; H 4.75; N 18.01.

5-(4-Bromophenyl)-3-phenyl-1,2,4-triazine (**6b**). Yield 53%, yellow powder. Mp 169–171 °C (from ethanol-acetone mixture 2: 1) (Lit. [30] mp 168–172 °C). ^{1}H NMR (400 MHz, DMSO-d_6/CCl_4), δ, ppm (*J*, Hz): 7.62-7.66 (3H, m, Ph); 7.83–7.90 (2H, m, 4-Br-C_6H_4); 8.39–8.45 (2H, m, 4-Br-C_6H_4); 8.55–8.58 (2H, m, Ph); 10.05 (1H, s, H-6). EI-MS (70 eV), *m/z* (Irel (%)): 313 $[M+1]^+$ (3), 311 (3), 182 (98), 180 (100), 102 (10), 101 (52), 75 (24). Found, %: C 57.92; H 3.34; N 13.21. $C_{15}H_{10}BrN_3$. Calculated, %: C 57.71; H 3.23; N 13.46.

5-(3,4-Dimethylphenyl)-3-phenyl-1,2,4-triazine (**6e**). Yield 56%, light yellow crystals. Mp 126–127 °C (from EtOH). ^{1}H NMR (400 MHz, DMSO-d_6), δ, ppm (*J*, Hz): 2.35 (3H, s, CH_3); 2.38 (3H, s, CH_3); 7.42 (1H, d, H-5′, 3,4-dimethylphenyl, *J* = 7.9); 7.60–7.67 (3H, m, Ph); 8.21 (1H, dd, H-6′, 3,4-dimethylphenyl, *J* = 7.9, 1.2); 8.27 (1H, d, H-2′, 3,4-dimethylphenyl, *J* = 1.2); 8.56–8.59 (2H, m, Ph); 10.00 (1H, s, H-6). EI-MS (70 eV), *m/z* (Irel (%)): 262 $[M+1]^+$ (2), 261 $[M]^{+\cdot}$ (7), 131 (12), 130 (100), 129 (18), 128 (10), 115 (42), 75 (24). Found, %: C 78.10; H 5.83; N 15.96. $C_{17}H_{15}N_3$. Calculated, %: C 78.13; H 5.79; N 16.08.

3-Phenyl-5-(thiophen-2-yl)-1,2,4-triazine (**6h**). Yield 60%, light yellow crystals. Mp 120–121 °C (from EtOH). ^{1}H NMR (400 MHz, DMSO-d_6), δ, ppm (*J*, Hz): 7.36–7.41 (1H, m, thiophen-2-yl); 7.63–7.65 (2H, m, Ph); 8.05–8.12 (1H, m, thiophen-2-yl); 8.37–8.42 (3H, m, thiophen-2-yl); 8.46–8.49 (1H, m, Ph); 9.94 (1H, s, H-6). EI-MS (70 eV), *m/z* (Irel (%)): 239 $[M]^{+\cdot}$ (7), 109 (8), 108 (100), 69 (10), 58 (8), 45 (9). Found, %: C 65.32; H 3.81; N 17.51. $C_{13}H_9N_3S$. Calculated, %: C 65.25; H 3.79; N 17.56.

5-(4-Bromophenyl)-3-(*p*-tolyl)-1,2,4-triazine (**7b**). Yield 50%, yellow powder. Mp 180–182 °C (from MeCN). ^{1}H NMR (400 MHz, DMSO-d_6), δ, ppm (*J*, Hz): 2.43 (3H, s, 4-CH_3-C_6H_4); 7.40–7.46 (2H, m, 4-CH_3-C_6H_4); 7.84–7.89 (2H, m, 4-Br-C_6H_4); 8.38–8.44 (2H, m, 4-Br-C_6H_4); 8.42–8.49 (2H, m, 4-CH_3-C_6H_4); 10.02 (1H, s, H-6). EI-MS (70 eV), *m/z* (Irel (%)): 327 $[M+1]^+$ (5), 325 (5), 183 (9), 180 (100), 182 (95), 181 (9), 180 (100), 101 (43), 75 (19). Found, %: C 59.03; H 3.82; N 12.67. $C_{16}H_{12}BrN_3$. Calculated, %: C 58.91; H 3.71; N 12.88.

5-(3,4-Dimethylphenyl)-3-(*p*-tolyl)-1,2,4-triazine (**7e**). Yield 63%, yellow crystals. Mp 171–173 °C (from EtOH). ^{1}H NMR (400 MHz, DMSO-d_6), δ, ppm (*J*, Hz): 2.34 (3H, s, CH_3); 2.37 (3H, s, CH_3); 2.43 (3H, s, CH_3); 2.48 (3H, s, CH_3); 7.40 (1H, d, H-5′, 3,4-dimethylphenyl, *J* = 8.1); 7.41–7.45 (2H, m, 4-CH_3-C_6H_4); 8.19 (1H, dd, H-6′, 3,4-dimethylphenyl, *J* = 8.1, 1.0); 8.24 (1H, d, H-2′, 3,4-dimethylphenyl, *J* = 1.0); 8.44–8.48 (2H, m, 4-CH_3-C_6H_4); 9.94 (1H, s, H-6). EI-MS (70 eV), *m/z* (Irel (%)): 276 $[M+1]^+$ (1), 275 $[M]^{+\cdot}$ (7), 131 (11), 130 (100), 129 (18), 128 (9), 116 (8), 115 (36). Found, %: C 78.54; H 6.28; N 15.24. $C_{18}H_{17}N_3$. Calculated, %: C 78.52; H 6.22; N 15.26.

5-(4-Methoxyphenyl)-3-(*p*-tolyl)-1,2,4-triazine (**7f**). Yield 63%, light yellow crystals. Mp 165–167 °C (from EtOH). ^{1}H NMR (400 MHz, DMSO-d_6), δ, ppm (*J*, Hz): 2.43 (3H, s, 4-CH_3-C_6H_4); 3.89 (3H, s, 4-CH_3O-C_6H_4); 7.15–7.21 (2H, m, Ar); 7.39–7.45 (2H, m, Ar); 8.41–8.47 (4H, m, Ar); 9.93 (1H, s, H-6). EI-MS (70 eV), *m/z* (Irel (%)): 278 $[M+1]^+$ (2), 277 $[M]^{+\cdot}$ (8), 133 (11), 132 (100), 117 (18), 89 (19). Found, %: C 73.70; H 5.48; N 15.12. $C_{17}H_{15}N_3O$. Calculated, %: C 73.63; H 5.45; N 15.15.

3,5-Di(thiophen-2-yl)-1,2,4-triazine (**8h**). Yield (59%, light yellow crystals. Mp 137–138 °C (from EtOH). ^{1}H NMR (400 MHz, DMSO-d_6), δ, ppm (*J*, Hz): 7.24–7.29 (m, 1H, thiophen-2-yl); 7.29–7.35 (m, 1H, thiophen-2-yl); 7.77–7.83 (m, 1H, thiophen-2-yl); 7.93–7.99 (m, 1H, thiophen-2-yl); 8.08–8.14 (m, 1H, thiophen-2-yl); 8.29–8.35 (m, 1H, Th); 9.75 (1H, s, H-6). EI-MS (70 eV), *m/z* (Irel (%)): 245 $[M]^{+\cdot}$ (11), 108 (100), 69 (13), 58 (13), 45 (15). Found, %: C 58.87; H 2.90; N 17.04. $C_{11}H_7N_3S_2$. Calculated, %: C 53.85; H 2.88; N 17.13.

3-(4-Chlorophenyl)-5-phenyl-1,2,4-triazine (**9a**). Yield 35%, yellow powder. Mp 118–120 °C (from ethanol) (Lit. [29,30] mp 118–123 °C). ^{1}H NMR (400 MHz, DMSO-d_6), δ, ppm (*J*, Hz): 7.63–7.73 (5H, m, Ph, 4-Cl-C_6H_4); 8.46–8.50 (2H, m, Ph); 10.07 (1H, s, H-6). EI-MS (70 eV), *m/z* (Irel (%)): 269 $[M+1]^+$ (1), 267 (5), 103 (9), 102 (100), 76 (8), 75 (3). Found, %: C 67.10; H 3.68; N 15.94. $C_{15}H_{10}ClN_3$. Calculated, %: C 67.30; H 3.77; N 15.70.

Triazines **6d, 6f, 6g, 7a, 7c, 7g, 8a, 8f, 8g** containing after recrystallization the regioisomer (3,6-disubstituted 1,2,4-triazines) as an impurity in an amount of up to 10% were used to prepare the corresponding 1,2,4-triazinium salts without further purification.

2.1.3. Preparation of 1-ethyl-3-R^1-5-R^2-1,2,4-triazin-1-ium Tetrafluoroborate **10–13** (General Method)

To a solution of triethyloxonium tetrafluoroborate (1.3 mmol) in absolute dichloroethane (2 mL), 3-R^1-5-R^2-1,2,4-triazine (1 mmol) was added. The reaction mixture was stirred at room temperature for 1–3 h. The precipitate of 1-ethyl-3-R^1-5-R^2-1,2,4-triazin-1-ium tetrafluoroborate was filtered off and recrystallized from absolute ethanol (see Supplementary Materials Figures S6–S21 for the ^{1}H NMR of compounds **10–13**).

1-Ethyl-3,5-diphenyl-1,2,4-triazin-1-ium tetrafluoroborate (**10a**). Yield 81%, light yellow powder. Mp 204 °C with dec. ^{1}H NMR (400 MHz, DMSO-d_6), δ, ppm (*J*, Hz): 1.81 (3H, t, NCH_2CH_3, *J* = 7.3); 4.93 (2H, q, NCH_2CH_3, *J* = 7.3); 7.70–7.90 (6H, m, Ph); 8.59–8.60 (4H, m, Ph); 10.69 (1H, s, H-6). Found, %: C 58.65; H 4.74; N 11.82. $C_{17}H_{16}BF_4N_3$. Calculated, %: C 58.48; H 4.62; N 12.04.

1-Ethyl-3-phenyl-5-(4-bromophenyl)-1,2,4-triazin-1-ium tetrafluoroborate (**10b**). Yield 72%, beige powder. Mp 207 °C with dec. ^{1}H NMR (400 MHz, DMSO-d_6), δ, ppm (*J*, Hz): 1.75 (3H, t, NCH_2CH_3, *J* = 7.3); 4.93 (2H, q, NCH_2CH_3, *J* = 7.3); 7.72–7.76 (2H, m, Ph); 7.81–7.83 (1H, m, Ph); 8.01–8.05 (2H, m, 4-Br-C_6H_4); 8.49–8.54 (2H, m, 4-Br-C_6H_4); 8.56–8.59 (2H, m, Ph); 10.72 (1H, s, H-6). Found, %: C 47.92; H 3.65; N 9.78. $C_{17}H_{15}BBrF_4N_3$. Calculated, %: C 47.70; H 3.53; N 9.82.

1-Ethyl-3-phenyl-5-(*p*-tolyl)-1,2,4-triazin-1-ium tetrafluoroborate (**10d**). Yield 91%, yellow powder. Mp 199 °C with dec. ^{1}H NMR (400 MHz, DMSO-d_6), δ, ppm (*J*, Hz): 1.80 (3H, t, NCH_2CH_3, *J* = 7.3); 2.56 (3H, s, 4-CH_3-C_6H_4); 4.90 (2H, q, NCH_2CH_3, *J* = 7.3); 7.56–7.61 (2H, m, 4-CH_3-C_6H_4); 7.69–7.72 (2H, m, Ph); 7.76–7.80 (1H, m, Ph); 8.47–8.53 (2H, m, 4-CH_3-C_6H_4); 8.57–8.58 (2H, m, Ph); 10.61 (1H, s, H-6). Found, %: C 59.75; H 5.14; N 11.52. $C_{18}H_{18}BF_4N_3$. Calculated, %: C 59.53; H 5.00; N 11.57.

5-(3,4-Dimethylphenyl)-1-ethyl-3-phenyl-1,2,4-triazin-1-ium tetrafluoroborate (**10e**). Yield 88%, bright yellow powder. Mp 198 °C with dec. ^{1}H NMR (400 MHz, DMSO-d_6), δ, ppm (*J*, Hz): 1.75 (3H, t, NCH_2CH_3, *J* = 7.3); 2.45 (6H, s, CH_3); 4.89 (2H, q, NCH_2CH_3, *J* = 7.3); 7.58 (1H, d, H-5′, 3,4-dimethylphenyl, *J* = 7.5); 7.72–7.76 (2H, m, Ph); 7.80–7.83 (1H, m, Ph); 8.35 (1H, br d, H-6′, 3,4-dimethylphenyl, *J* = 7.5); 8.40 (1H, br s, H-2′, 3,4-dimethylphenyl); 8.58-8.59 (2H, m, Ph); 10.62 (1H, s, H-6). Found, %: C 60.72; H 5.48; N 10.98. $C_{19}H_{20}BF_4N_3$. Calculated, %: C 60.50; H 5.34; N 11.14.

1-Ethyl-5-(4-methoxyphenyl)-3-phenyl-1,2,4-triazin-1-ium tetrafluoroborate (**10f**). Yield 91%, bright yellow crystals. Mp 188–190 °C. ^{1}H NMR (400 MHz, DMSO-d_6), δ, ppm (*J*,

Hz): 1.74 (3H, t, NCH_2CH_3, *J* = 7.2); 3.99 (3H, s, 4-CH_3O-C_6H_4); 4.85 (2H, q, NCH_2CH_3, *J* = 7.2); 7.31–7.39 (2H, m, 4-CH_3O-C_6H_4); 7.71–7.80 (3H, m, Ph); 8.49–8.65 (4H, m, Ph, 4-CH_3O-C_6H_4); 10.57 (1H, s, H-6). Found, %: C 57.22; H 4.98; N 10.95. $C_{18}H_{18}BF_4N_3O$. Calculated, %: C 57.02; H 4.79; N 11.08.

1-Ethyl-5-(naphthalen-2-yl)-3-phenyl-1,2,4-triazin-1-ium tetrafluoroborate (**10g**). Yield 71%, light orange powder. Mp 193 °C with dec. ^{1}H NMR (400 MHz, DMSO-d_6), δ, ppm (*J*, Hz): 1.79 (3H, t, NCH_2CH_3, *J* = 7.2); 4.94 (2H, q, NCH_2CH_3, *J* = 7.2), 7.70–7.88 (5H, m, Ar); 8.11–8.19 (1H, m, Ar); 8.22–8.36 (2H, m, Ar); 8.64–8.66 (3H, m, Ar); 9.26–9.37 (1H, m, Ar); 10.83 (1H, s, H-6). Found, %: C 63.22; H 4.72; N 10.35. $C_{21}H_{18}BF_4N_3$. Calculated, %: C 63.18; H 4.54; N 10.53.

1-Ethyl-3-phenyl-5-(thiophen-2-yl)-1,2,4-triazin-1-ium tetrafluoroborate (**10h**). Yield 70%, yellow powder. Mp 190 °C with dec. ^{1}H NMR (400 MHz, DMSO-d_6), δ, ppm (*J*, Hz): 1.74 (3H, t, NCH_2CH_3, *J* = 7.2); 4.82 (2H, q, NCH_2CH_3, *J* = 7.2); 7.55–7.61 (1H, m, thiophen-2-yl); 7.68–7.70 (2H, m, Ph); 7.75–7.77 (1H, m, Ph); 8.38–8.49 (1H, m, thiophen-2-yl); 8.45–8.46 (2H, m, Ph); 8.54–8.60 (1H, m, thiophen-2-yl); 10.54 (1H, s, H-6). Found, %: C 50.92; H 4.05; N 11.75. $C_{15}H_{14}BF_4N_3S$. Calculated, %: C 50.73; H 3.97; N 11.83.

1-Ethyl-5-phenyl-3-(*p*-tolyl)-1,2,4-triazin-1-ium tetrafluoroborate (**11a**). Yield 79%, light yellow powder. Mp 186 °C with dec. ^{1}H NMR (400 MHz, DMSO-d_6), δ, ppm (*J*, Hz): 1.75 (3H, t, NCH_2CH_3, *J* = 7.1), 4.89 (2H, q, NCH_2CH_3, *J* = 7.1), 7.52–7.58 (2H, m, 4-CH_3-C_6H_4); 7.79–7.82 (2H, m, Ph); 7.88–7.90 (1H, m, Ph); 8.45–8.52 (2H, m, 4-CH_3-C_6H_4); 8.58–8.60 (1H, m, Ph); 10.65 (1H, s, H-6). Found, %: C 59.66; H 5.14; N 11.42. $C_{18}H_{18}BF_4N_3$. Calculated, %: C 59.53; H 5.00; N 11.58.

5-(4-Bromophenyl)-1-ethyl-3-(*p*-tolyl)-1,2,4-triazin-1-ium tetrafluoroborate (**11b**). Yield 74%, light yellow powder. Mp 190 °C with dec. ^{1}H NMR (400 MHz, DMSO-d_6), δ, ppm (*J*, Hz): 1.74 (3H, t, NCH_2CH_3, *J* = 7.2); 2.49 (3H, s, CH_3); 4.88 (2H, q, NCH_2CH_3, *J* = 7.2); 7.54–7.56 (2H, m, Ar); 8.04–8.06 (2H, m, Ar); 8.47–8.52 (4H, m, Ar); 10.67 (1H, s, H-6). Found, %: C 49.12; H 3.95; N 9.38. $C_{18}H_{17}BBrF_4N_3$. Calculated, %: C 48.91; H 3.88; N 9.51.

5-(3,4-Dimethylphenyl)-1-ethyl-3-(*p*-tolyl)-1,2,4-triazin-1-ium tetrafluoroborate (**11e**). Yield 93%, bright yellow powder. Mp 204 °C with dec. ^{1}H NMR (400 MHz, DMSO-d_6), δ, ppm (*J*, Hz): 1.74 (3H, t, NCH_2CH_3, *J* = 7.2); 2.42 (3H, s, CH_3); 2.44 (3H, s, CH_3); 2.48 (3H, s, CH_3); 4.85 (2H, q, NCH_2CH_3, *J* = 7.2); 7.51–7.57 (2H, m, 4-CH_3-C_6H_4); 7.57 (1H, d, H-5′, 3,4-dimethylphenyl, *J* = 8.1); 8.33 (1H, dd, H-6′, 3,4-dimethylphenyl, *J* = 8.1, 1.0); 8.38 (1H, d, H-2′, 3,4-dimethylphenyl, *J* = 1.0); 8.45–8.50 (2H, m, 4-CH_3-C_6H_4); 10.56 (1H, s, H-6). Found, %: C 61.52; H 5.70; N 10.67. $C_{20}H_{22}BF_4N_3$. Calculated, %: C 61.40; H 5.67; N 10.74.

1-Ethyl-5-(4-methoxyphenyl)-3-(*p*-tolyl)-1,2,4-triazin-1-ium tetrafluoroborate (**11f**). Yield 87%, bright yellow crystals. Mp 194 °C with dec. ^{1}H NMR (400 MHz, DMSO-d_6), δ, ppm (*J*, Hz): 1.73 (3H, t, NCH_2CH_3, *J* = 7.1); 2.48 (3H, s, 4-CH_3-C_6H_4); 3.98 (3H, s, OCH_3); 4.83 (2H, q, NCH_2CH_3, *J* = 7.1); 7.30–7.38 (2H, m, 4-CH_3O-C_6H_4); 7.50–7.56 (2H, m, 4-CH_3-C_6H_4); 8.40–8.49 (2H, m, 4-CH_3-C_6H_4); 8.54–8.62 (2H, m, 4-CH_3O-C_6H_4). 10.52 (1H, s, H-6). Found, %: C 58.14; H 5.08; N 10.67. $C_{19}H_{20}BF_4N_3O$. Calculated, %: C 58.04; H 5.13; N 10.69.

1-Ethyl-5-(naphthalen-2-yl)-3-(*p*-tolyl)-1,2,4-triazin-1-ium tetrafluoroborate (**11g**). Yield 87%, bright yellow powder. Mp 191 °C with dec. ^{1}H NMR (400 MHz, DMSO-d_6), δ, ppm (*J*, Hz): 1.78 (3H, t, NCH_2CH_3, *J* = 7.1); 2.51 (3H, s, 4-CH_3-C_6H_4); 4.92 (2H, q, NCH_2CH_3, *J* = 7.1), 7.52–7.64 (2H, m, 4-CH_3-C_6H_4); 7.74–7.85 (2H, m, naphthalen-2-yl); 8.14–8.16 (1H, m, naphthalen-2-yl); 8.25–8.32 (2H, m, naphthalen-2-yl); 8.48–8.66 (3H, m, 4-CH_3–C_6H_4 (2H), naphthalen-2-yl(1H)); 9.24–9.33 (1H, m, naphthalen-2-yl,); 10.78 (1H, s, H-6). Found, %: C 63.98; H 4.92; N 10.12. $C_{22}H_{20}BF_4N_3$. Calculated, %: C 63.95; H 4.88; N 10.17.

1-Ethyl-5-phenyl-3-(thiophen-2-yl)-1,2,4-triazin-1-ium tetrafluoroborate (**12a**). Yield 89%, orange powder. Mp 190 °C with dec. ^{1}H NMR (400 MHz, DMSO-d_6), δ, ppm (*J*, Hz): 1.71 (3H, t, NCH_2CH_3, *J* = 7.1); 4.83 (2H, q, NCH_2CH_3, *J* = 7.1); 7.42–7.49 (1H, m, thiophen-2-yl); 7.75–7.95 (3H, m, Ph); 8.19–8.27 (1H, m, thiophen-2-yl); 8.38–8.58 (3H, m, thiophen-2-yl (1H), Ph (2H)); 10.56 (1H, s, H-6). Found, %: C 50.86; H 4.02; N 11.72. $C_{15}H_{14}BF_4N_3S$. Calculated, %: C 50.73; H 3.97; N 11.83.

1-Ethyl-5-(4-methoxyphenyl)-3-(thiophen-2-yl)-1,2,4-triazin-1-ium tetrafluoroborate (**12f**). Yield 87%, orange powder. Mp 185 °C with dec. ^{1}H NMR (400 MHz, DMSO-d_6), δ, ppm (*J*, Hz): 1.69 (3H, t, NCH_2CH_3, *J* = 7.2); 3.98 (3H, s, OCH_3); 4.77 (2H, q, NCH_2CH_3, *J* = 7.2); 7.31–7.39 (2H, m, 4-CH_3O-C_6H_4); 7.40–7.47 (1H, m, thiophen-2-yl); 8.16–8.23 (1H, m, thiophen-2-yl); 8.35–8.41 (1H, m, thiophen-2-yl); 8.47–8.56 (2H, m, 4-CH_3O-C_6H_4); 10.44 (1H, s, H-6). Found, %: C 49.98; H 4.22; N 10.82. $C_{16}H_{16}BF_4N_3OS$. Calculated, %: C 49.89; H 4.19; N 10.91.

1-Ethyl-5-(naphthalen-2-yl)-3-(thiophen-2-yl)-1,2,4-triazin-1-ium tetrafluoroborate **(12g)**. Yield 97%, orange powder. Mp 193–195 °C. ^{1}H NMR (400 MHz, DMSO-d_6), δ, ppm (*J*, Hz): 1.74 (3H, t, NCH_2CH_3, *J* = 6.8); 4.85 (2H, q, NCH_2CH_3, *J* = 6.8), 7.45–7.50 (1H, m, thiophen-2-yl); 7.73–7.88 (2H, m, naphthalen-2-yl); 8.11–8.19 (1H, m); 8.19–8.27 (2H, m); 8.27–8.34 (1H, m); 8.46–8.58 (2H, m, naphthalen-2-yl); 9.18–9.28 (1H, m, naphthalen-2-yl,); 10.69 (1H, s, H-6). Found, %: C 56.44; H 4.05; N 10.11. $C_{19}H_{16}BF_4N_3$**S**. Calculated, %: C 56.32; H 3.98; N 10.37.

1-Ethyl-3,5-di(thiophen-2-yl)-1,2,4-triazin-1-ium tetrafluoroborate (**12h**). Yield 94%, yellow powder. Mp 191 °C with dec. ^{1}H NMR (400 MHz, DMSO-d_6), δ, ppm (*J*, Hz): 1.72 (3H, t, NCH_2CH_3, *J* = 7.2); 4.74 (2H, q, NCH_2CH_3, *J* = 7.2); 7.35–7.42 (1H, m, thiophen-2-yl); 7.48–7.55 (1H, m, thiophen-2-yl); 8.09–8.15 (1H, m, thiophen-2-yl); 8.23–8.29 (1H, m, thiophen-2-yl); 8.33–8.41 (1H, m, thiophen-2-yl), 8.50–8.56 (1H, m, thiophen-2-yl), 10.39 (1H, s, H-6). Found, %: C 43.28; H 3.32; N 10.51. $C_{13}H_{12}BF_4N_3S_2$. Calculated, %: C 43.23; H 3.35; N 11.63.

3-(4-Chlorophenyl)-1-ethyl-5-phenyl-1,2,4-triazin-1-ium tetrafluoroborate (**13a**). Yield 62%, beige powder. Mp 193 °C with dec. ^{1}H NMR (400 MHz, acetone-d_6), δ, ppm (*J*, Hz): 1.93 (3H, t, NCH_2CH_3, *J* = 6.8), 5.21 (2H, q, NCH_2CH_3, *J* = 6.8), 7.78–7.81 (6H, m, Ph, 4-Cl-C_6H_4); 7.89–7.93 (1H, m, Ph); 8.66–8.69 (2H, m, Ph); 10.63 (1H, s, H-6). Found, %: C 53.20; H 4.00; N 11.82. $C_{17}H_{15}BClF_4N_3$. Calculated, %: C 53.23; H 3.94; N 10.95.

2.1.4. Preparation of Dimethyl 7-methyl-2-R^2-4-R^1-pyrrolo[2,1-*f*][1,2,4]triazine-5,6-dicarboxylate **14**–**17** (General Method)

To a suspension of N(1)-ethyl-1,2,4-triazinium tetrafluoroborate (1.0 mmol) in dry tetrahydrofuran (or absolute dioxane), first dimethyl acetylenedicarboxylate (1.2 mmol) was added, then triethylamine (1.1 mmol) dropwise under stirring. The reaction mixture was stirred at room temperature until a crystalline product precipitated, which was separated by filtration and recrystallized. If the precipitate did not form within two days, the solvent was evaporated, the product was suspended in methanol, then filtered off and recrystallized (see Supplementary Materials Figures S22–S39 for the ^{1}H NMR, ^{13}C NMR, and mass spectra data of compounds **14**–**17**).

Dimethyl 7-methyl-2,4-diphenylpyrrolo[2,1-*f*][1,2,4]triazine-5,6-dicarboxylate (**14a**). Reaction conditions: 0.8 mL absolute dioxane, reaction time 4 days. Yield 30%, yellow powder. Mp 206–208 °C (from CH_3CN). ^{1}H NMR (600 MHz, DMSO-d_6), δ, ppm (*J*, Hz): 2.90 (3H, s, 7-CH_3); 3.40 (3H, s, CO_2CH_3); 3.86 (3H, s, CO_2CH_3); 7.53–7.54 (3H, m, Ph); 7.57–7.60 (2H, m, Ph); 7.62–7.65 (1H, m, Ph); 7.72–7.75 (2H, m, Ph); 8.40–8.43 (2H, m, Ph). ^{13}C NMR (101 MHz, DMSO-d_6), t = 50 °C, δ, ppm: 10.5; 52.4; 52.5; 112.8; 116.5; 117.9; 127.9; 128.7; 128.9; 129.2; 131.5; 131.6; 134.9; 136.5; 154.7; 162.6; 163.9; 164.6. EI-MS (70 eV), *m/z* (Irel (%)): 402 $[M+1]^+$ (27), 401 $[M]^{+\cdot}$(100), 370 (26), 369 (71), 338 (30), 337 (32), 283 (16), 282 (34), 281 (21), 152 (19), 151 (13), 126 (13), 77 (24). Found, %: C 68.75; H 4.70; N 10.51. $C_{23}H_{19}N_3O_4$. Calculated, %: C 68.82; H 4.77; N 10.47.

Dimethyl 4-(4-bromophenyl)-7-methyl-2-phenylpyrrolo[2,1-*f*][1,2,4]triazine-5,6-dicarboxylate (**14b**). Reaction conditions: 2.5 mL absolute dioxane, reaction time: 2 days. Yield 54%, yellow powder. Mp 155–157 °C (from EtOH). ^{1}H NMR (400 MHz, DMSO-d_6), δ, ppm (*J*, Hz): 2.84 (3H, s, 7-CH_3); 3.49 (3H, s, CO_2CH_3); 3.84 (3H, s, CO_2CH_3); 7.53–7.62 (3H, m, Ph); 7.64–7.71 (2H, m, 4-Br-C_6H_4); 7.79–7.85 (2H, m, 4-Br-C_6H_4); 8.33–8.43 (2H, m, Ph). ^{13}C NMR (101 MHz, DMSO-d_6), δ, ppm: 10.5; 52.6; 52.7; 112.4; 116.5; 117.7; 125.3; 127.8; 129.2; 130.7; 131.6; 131.7; 131.9 134.6; 135.5; 154.4; 161.3; 163.8; 164.7. EI-MS (70 eV), *m/z* (Irel

(%)): 482 $[M+2]^+$ (16), 481 $[M+1]^+$ (59), 480 $[M]^{+\cdot}$(20), 479 (59), 449 (61), 447 (60), 362 (30), 360 (28), 152 (35), 151 (45), 150 (67), 125 (25), 104 (51), 103 (36), 77 (100). Found, %: C 57.48; H 3.84; N 8.64. $C_{23}H_{18}BrN_3O_4$. Calculated, %: C 57.51; H 3.78; N 8.75.

Dimethyl 7-methyl-2-phenyl-4-(*p*-tolyl)pyrrolo[2,1-*f*][1,2,4]triazine-5,6-dicarboxylate (**14d**). Reaction conditions: 2.5 mL absolute dioxane, reaction time 4 days. Yield 53%, light orange crystals. Mp 191–192 °C (from CH_3CN). ^{1}H NMR (400 MHz, DMSO-d_6), δ, ppm (*J*, Hz): 2.44 (3H, s, 4-CH_3-C_6H_4); 2.84 (3H, s, 7-CH_3); 3.46 (3H, s, CO_2CH_3); 3.84 (3H, s, CO_2CH_3); 7.37–7.43 (2H, m, 4-CH_3-C_6H_4); 7.55–7.60 (3H, m, Ph); 7.63–7.68 (2H, m, 4-CH_3-C_6H_4); 8.38–8.42 (2H, m, Ph). ^{13}C NMR (101 MHz, DMSO-d_6), t = 50 °C, δ, ppm: 10.5; 21.5; 52.47; 52.50; 112.8; 116.4; 117.8; 127.9; 128.7; 129.2; 129.4; 131.45; 131.54; 133.8; 135.0; 141.7; 154.6; 162.4; 163.9; 164.8. EI-MS (70 eV), *m/z* (Irel (%)): 416 $[M+1]^+$ (29), 415 $[M]^+$(100), 384 (20), 383 (42), 368 (19), 352 (44), 351 (53), 296 (34), 295 (36), 165 (24), 139 (19), 104 (16), 77 (34). Found, %: C, 69.42; H 5.24; N 10.04. $C_{24}H_{21}N_3O_4$. Calculated, %: C 69.39; H 5.10; N 10.11.

Dimethyl 4-(3,4-dimethylphenyl)-7-methyl-2-phenylpyrrolo[2,1-*f*][1,2,4]triazine-5,6-dicarboxylate (**14e**). Reaction conditions: 3.0 mL dry tetrahydrofuran, reaction time 4 days. Yield 44%, yellow powder. Mp 203–205 °C (from EtOH). ^{1}H NMR (400 MHz, DMSO-d_6), δ, ppm (*J*, Hz): 2.34 (3H, s, CH_3-C_6H_4); 2.36 (3H, s, CH_3-C_6H_4); 2.86 (3H, s, 7-CH_3); 3.47 (3H, s, CO_2CH_3); 3.84 (3H, s, CO_2CH_3); 7.36 (1H, d, H-5′, 3,4-dimethylphenyl, *J* = 7.6); 7.51 (1H, dd, H-6′, 3,4-dimethylphenyl, *J* = 7.6; 1.6); 7.54 (1H, d, H-2′, 3,4-dimethylphenyl, *J* = 1.6); 7.56–7.61 (3H, m, Ph); 8.40–8.42 (2H, m, Ph). ^{13}C NMR (101 MHz, DMSO-d_6), t = 50 °C, δ, ppm: 10.5; 19.77; 19.84; 52.5; 112.8; 116.3; 117.8; 126.3; 128.0; 129.2; 129.7; 130.0; 131.5; 134.1; 135.1; 136.9; 140.5; 154.7; 162.5; 163.9; 164.9. EI-MS (70 eV), *m/z* (Irel (%)): 430 $[M+1]^+$ (30), 429 $[M]^+$ (100), 414 (17), 398 (14), 397 (25), 382 (43), 366 (44), 365 (59), 310 (23), 309 (26), 165 (13), 104 (16), 103 (17), 77 (33). Found, %: C 69.96; H 5.29; N 9.71. $C_{25}H_{23}N_3O_4$. Calculated, %: C 69.92; H 5.40; N 9.78.

Dimethyl 4-(4-methoxyphenyl)-7-methyl-2-phenylpyrrolo[2,1-*f*][1,2,4]triazine-5,6-dicarboxylate (**14f**). Reaction conditions: 3.0 mL dry tetrahydrofuran, reaction time 4 days. Yield 64%, yellow powder. Mp 202–204 °C (from CH_3CN). ^{1}H NMR (400 MHz, DMSO-d_6), δ, ppm (*J*, Hz): 2.85 (3H, s, 7-CH_3); 3.54 (3H, s, CO_2CH_3); 3.85 (3H, s, CH_3); 3.89 (3H, s, CH_3); 7.12–7.18 (2H, m, 4-CH_3O-C_6H_4); 7.51–7.62 (3H, m, Ph); 7.69–7.79 (2H, m, 4-CH_3O-C_6H_4); 8.35–8.44 (2H, m, Ph). ^{13}C NMR (101 MHz, DMSO-d_6), δ, ppm: 10.6; 52.6; 52.8; 56.0; 112.7; 114.4; 116.2; 117.7; 127.9; 128.8; 129.3; 130.7; 131.5; 135.0; 154.5; 161.8; 162.4; 164.0; 165.0. EI-MS (70 eV), *m/z* (Irel (%)): 432 $[M+1]^+$ (30), 431 $[M]^{+\cdot}$(100), 416 (17), 400 (16), 399 (29), 368 (35), 367 (30), 312 (19), 183 (14), 170 (14), 77 (33). Found, %: C 66.76; H 4.88; N 9.72. $C_{24}H_{21}N_3O_5$. Calculated, %: C 66.81; H 4.91; N 9.74.

Dimethyl 7-methyl-4-(naphthalen-2-yl)-2-phenylpyrrolo[2,1-*f*][1,2,4]triazine-5,6-dicarboxylate (**14g**). Reaction conditions: 3.0 mL dry tetrahydrofuran, reaction time 4 days. Yield 58%, orange-colored fine crystalline powder. Mp 200–202 °C (from CH_3CN). ^{1}H NMR (400 MHz, DMSO-d_6), δ, ppm (*J*, Hz): 2.89 (3H, s, 7-CH_3); 3.28 (3H, s, CO_2CH_3); 3.85 (3H, s, CO_2CH_3); 7.53–7.63 (3H, m, Ph); 7.63–7.74 (2H, m, naphthalen-2-yl); 7.90 (1H, dd, H-3′, naphthalen-2-yl, *J* = 8.1; 1.2); 8.01–8.11 (2H, m, naphthalen-2-yl); 8.15 (1H, d, H-4′, naphthalen-2-yl, *J* = 8.1); 8.33 (1H, d, H-1′, naphthalen-2-yl, *J* = 1.2); 8.41–8.48 (2H, m, Ph). ^{13}C NMR (101 MHz, DMSO-d_6), δ, ppm: 10.6; 52.6; 52.7; 112.8; 116.5; 118.0; 127.5; 128.0; 128.3; 128.8; 129.2; 129.3; 131.7; 132.5; 133.8; 134.5; 134.9; 154.6; 162.4; 163.9; 164.9. EI-MS (70 eV), *m/z* (Irel (%)): 452 $[M+1]^+$ (31), 451 $[M]^{+\cdot}$(100), 388 (32), 387 (45), 332 (15), 331 (23), 202 (11), 127 (10), 77 (33). Found, %: C 71.68; H 4.61; N 9.28. $C_{27}H_{21}N_3O_4$. Calculated, %: C 71.83; H 4.69; N 9.31.

Dimethyl 7-methyl-2-phenyl-4-(thiophen-2-yl)pyrrolo[2,1-*f*][1,2,4]triazine-5,6-dicarboxylate (**14h**). Reaction conditions: 2.0 mL dry tetrahydrofuran, reaction time 4 days. Yield 48%, bright orange crystalline powder. Mp 166–167 °C (from EtOH). ^{1}H NMR (600 MHz, DMSO-d_6), δ, ppm (*J*, Hz): 2.88 (3H, s, 7-CH_3); 3.71 (3H, s, CO_2CH_3); 3.89 (3H, s, CO_2CH_3); 7.28–7.30 (1H, m, thiophen-2-yl); 7.52–7.55 (3H, m, Ph); 7.58–7.60 (1H, m, thiophen-2-yl); 7.96–7.98 (1H, m, thiophen-2-yl); 8.37–8.39 (2H, m, Ph). ^{13}C NMR (101 MHz,

DMSO-d_6), t = 50 °C, δ, ppm: 10.6; 52.6; 53.0; 112.7; 116.4; 116.5; 127.8; 128.9; 129.2; 131.4; 131.6; 132.1; 133.4; 134.7; 139.4; 154.1; 155.2; 163.8; 165.5. EI-MS (70 eV), *m/z* (Irel (%)): 408 $[M+1]^+$ (25), 407 $[M]^+$ (100), 376 (35), 375 (86), 344 (16), 317 (20), 289 (26), 288 (15), 158 (26), 77 (15). Found, %: C 62.05; H 4.30; N 10.51. $C_{21}H_{17}N_3O_4S$. Calculated, %: C 61.90; H 4.21; N 10.31.

Dimethyl 7-methyl-4-phenyl-2-*p*-tolylpyrrolo[2,1-*f*][1,2,4]triazine-5,6-dicarboxylate (**15a**). Reaction conditions: 3 mL of absolute dioxane, reaction time 1 day. Yield 42%. Mp 179–180 °C (from EtOH). ^{1}H NMR (600 MHz, DMSO-d_6), t = 60 °C, δ, ppm (*J*, Hz): 2.36 (3H, s, CH_3-C_6H_4); 2.80 (3H, s, 7-CH_3); 3.41 (3H, s, CO_2CH_3); 3.83 (3H, s, CO_2CH_3); 7.28–7.32 (2H, m, CH_3-C_6H_4); 7.55–7.60 (2H, m, Ph); 7.61–7.66 (1H, m, Ph); 7.68–7.73 (2H, m, Ph); 8.19–8.24 (2H, m, CH_3-C_6H_4). ^{13}C NMR (151 MHz, DMSO-d_6), t = 60 °C, δ, ppm: 10.4; 21.4; 52.4; 112.7; 116.3; 117.8; 127.7; 128.6, 128.8; 129.7; 131.41; 131.44; 132.1; 136.6; 141.4; 154.6; 162.3; 163.9; 164.7. EI-MS (70 eV), *m/z* (Irel (%)): 416 $[M+1]^+$ (27), 415 $[M]^{+\cdot}$(100), 384 (28), 383 (63), 352 (32), 351 (30), 296 (54), 152 (61), 151 (42), 126 (44), 116 (45), 91 (45), 89 (31), 77 (48). Found, %: C 69.42; H 5.23; N 9.97. $C_{24}H_{21}N_3O_4$. Calculated, %: C 69.39; H 5.10; N 10.11.

Dimethyl 4-(4-bromophenyl)-7-methyl-2-*p*-tolylpyrrolo[2,1-*f*][1,2,4]triazine-5,6-dicarboxylate (**15b**). Reaction conditions: 3.0 mL absolute dioxane, reaction time 4 days. Yield 27%, bright yellow crystals. Mp 181–182 °C (from EtOH). ^{1}H NMR (400 MHz, DMSO-d_6), δ, ppm (*J*, Hz): 2.40 (3H, s, 4-CH_3-C_6H_4); 2.83 (3H, s, 7-CH_3); 3.48 (3H, s, CO_2CH_3); 3.84 (3H, s, CO_2CH_3); 7.33–7.40 (2H, m, 4-CH_3-C_6H_4); 7.63–7.70 (2H, m, 4-Br-C_6H_4); 7.79–7.84 (2H, m, 4-Br-C_6H_4); 8.24–8.30 (2H, m, 4-CH_3-C_6H_4). ^{13}C NMR (101 MHz, DMSO-d_6), δ, ppm: 10.5; 21.5; 52.6; 52.7; 112.4; 116.3; 117.6; 125.3; 127.7; 129.8; 130.7; 131.6; 131.8; 131.9; 135.6; 141.5; 154.4; 161.2; 163.9; 164.7. EI-MS (70 eV), *m/z* (Irel (%)): 496 $[M+2]^+$ (22), 495 $[M+1]^+$ (85), 494 $[M]^+$ (26), 493 (84), 464 (27), 463 (76), 462 (33), 461 (74), 432 (19), 377 (19), 376 (37), 375 (26), 374 (40), 77 (40). Found, %: C 58.24; H 4.10; N 8.52. $C_{24}H_{20}BrN_3O_4$. Calculated, %: C 58.31; H 4.08; N 8.50.

Dimethyl 4-(4-chlorophenyl)-7-methyl-2-*p*-tolylpyrrolo[2,1-*f*][1,2,4]triazine-5,6-dicarboxylate (**15c**). Reaction conditions: 3.0 mL dry tetrahydrofuran, reaction time 4 days. Yield 54%, bright yellow powder. Mp 182–183 °C (from CH_3CN). ^{1}H NMR (400 MHz, DMSO-d_6), δ, ppm (*J*, Hz): 2.39 (3H, s, CH_3-C_6H_4); 2.82 (3H, s, 7-CH_3); 3.49 (3H, s, CO_2CH_3); 3.84 (3H, s, CO_2CH_3); 7.32–7.38 (2H, m, 4-CH_3-C_6H_4); 7.64–7.70 (2H, m, 4-Cl-C_6H_4); 7.70–7.76 (2H, m, 4-Cl-C_6H_4); 8.22–8.28 (2H, m, 4-CH_3-C_6H_4). ^{13}C NMR (151 MHz, DMSO-d_6), t = 50 °C, δ, ppm: 10.4; 21.5; 52.5; 52.6; 112.5; 116.5; 117.7; 127.8; 129.0; 129.7; 130.5; 131.6; 132.0; 135.3; 136.5; 141.5; 154.6; 161.2; 163.9; 164.6. EI-MS (70 eV), *m/z* (Irel (%)): 452 (10), 451 $[M+2]^+$ (37), 450 $[M+1]^+$ (29), 449 $[M]^{+\cdot}$(100), 419 (38), 418 (40), 417 (100), 386 (23), 331 (27), 330 (45), 186 (19), 152 (22), 151 (31), 150 (35), 139 (210, 118 (33), 117 (19), 116 (39), 91 (44), 90 (23), 89 (24), 75 (17). Found, %: C 64.13; H 4.51; N 9.28. $C_{24}H_{20}ClN_3O_4$. Calculated, %: C 64.07; H 4.48; N 9.34.

Dimethyl 4-(3,4-dimethylphenyl)-7-methyl-2-*p*-tolylpyrrolo[2,1-*f*][1,2,4]triazine-5,6-dicarboxylate (**15e**). Reaction conditions: 2.5 mL dry tetrahydrofuran, reaction time 3 days. Yield 60%, yellow powder. Mp 178–179 °C (from CH_3CN). ^{1}H NMR (400 MHz, DMSO-d_6), δ, ppm (*J*, Hz): 2.33 (3H, s, CH_3); 2.35 (3H, s, CH_3); 2.40 (3H, s, CH_3), 2.83 (3H, s, 7-CH_3); 3.46 (3H, s, CO_2CH_3); 3.84 (3H, s, CO_2CH_3); 7.32–7.40 (3H, m, Ar); 7.46–7.53 (2H, m, Ar); 8.25–8.31 (2H, m, Ar). ^{13}C NMR (101 MHz, DMSO-d_6), t = 50 °C, δ, ppm: 10.5; 19.76; 19.84; 21.5; 52.5; 112.8; 116.2; 117.8; 126.2; 127.9; 129.7; 129.8; 130.0; 131.4; 132.3; 134.1; 136.8; 140.5; 141.4; 154.7; 162.4; 163.9; 164.9. EI-MS (70 eV), *m/z* (Irel (%)): 444 $[M+1]^+$ (30), 443 $[M]^+$ (100), 411 (22), 396 (43), 380 (41), 379 (51), 324 (30), 323 (30), 165 (27), 118 (29), 116 (48), 91 (60), 77 (29). Found, %: C 70.42; H 5.79; N 9.41. $C_{26}H_{25}N_3O_4$. Calculated, %: C 70.41; H 5.68; N 9.47.

Dimethyl 4-(4-methoxyphenyl)-7-methyl-2-*p*-tolylpyrrolo[2,1-*f*][1,2,4]triazine-5,6-dicarboxylate (**15f**). Reaction conditions: 2.5 mL dry tetrahydrofuran, reaction time 4 days. Yield 68%, light yellow powder. Mp 188–189 °C (from CH_3CN). ^{1}H NMR (400 MHz, DMSO-d_6), δ, ppm (*J*, Hz): 2.40 (3H, s, CH_3-C_6H_4); 2.82 (3H, s, 7-CH_3); 3.53 (3H, s, CO_2CH_3); 3.84

(3H, s, CH_3); 3.88 (3H, s, CH_3); 7.10–7.18 (2H, m, 4-CH_3O-C_6H_4); 7.34–7.39 (2H, m, 4-CH_3-C_6H_4); 7.71–7.77 (2H, m, 4-CH_3O-C_6H_4); 8.25–8.32 (2H, m, 4-CH_3-C_6H_4). ^{13}C NMR (101 MHz, DMSO-d_6), δ, ppm: 10.6; 21.5; 52.6; 52.8; 56.0; 112.6; 114.4; 116.0; 117.7; 127.8; 128.8; 129.8; 130.6; 131.4; 132.2; 141.4; 154.5; 161.7; 162.3; 164.0; 165.0. EI-MS (70 eV), *m/z* (Irel (%)): 446 $[M+1]^+$ (30), 445 $[M]^+$ (100), 430 (16), 414 (15), 413 (28), 382 (31), 381 (27), 326 (19), 325 (12), 223 (12). Found, %: C 67.43; H 5.22; N 9.41. $C_{25}H_{23}N_3O_5$. Calculated, %: C 67.41; H 5.20; N 9.43.

Dimethyl 7-methyl-4-(naphthalen-2-yl)-2-*p*-tolylpyrrolo[2,1-*f*][1,2,4]triazine-5,6-dicarboxylate (**15g**). Reaction conditions: 4.0 mL dry tetrahydrofuran, reaction time 4 days. Yield 52%, light orange colored fine crystalline powder. Mp 190–192 °C (from CH_3CN). ^{1}H NMR (400 MHz, DMSO-d_6), δ, ppm (*J*, Hz): 2.42 (3H, s, CH_3-C_6H_4); 2.88 (3H, s, 7-CH_3); 3.27 (3H, s, CO_2CH_3); 3.84 (3H, s, CO_2CH_3); 7.38–7.43 (2H, m, CH_3-C_6H_4); 7.62–7.72 (2H, m, naphthalen-2-yl) 8.28–8.40 (3H, m, CH_3-C_6H_4 (2H), naphthalen-2-yl (1H)). ^{13}C NMR (101 MHz, DMSO-d_6), δ, ppm: 10.6; 21.6; 52.56; 52.61; 112.7; 116.3; 118.0; 125.6; 127.9; 128.32; 128.34; 128.7; 129.1; 129.2; 129.9; 131.6; 132.1; 132.5; 133.8; 134.5; 141.6; 154.6; 162.3; 163.9; 164.9. EI-MS (70 eV), *m/z* (Irel (%)): 466 $[M+1]^+$ (33), 465 $[M]^{+\cdot}$(100), 450 (10), 402 (29), 401 (39), 346 (13), 345 (18), 202 (9). Found, %: C 72.08; H 4.92; N 9.05. $C_{28}H_{23}N_3O_4$. Calculated, %: C 72.24; H 4.98; N 9.03.

Dimethyl 7-methyl-4-phenyl-2-(thiophen-2-yl)pyrrolo[2,1-*f*][1,2,4]triazine-5,6-dicarboxylate (**16a**). Reaction conditions: 2.5 mL dry tetrahydrofuran, reaction time 4 days. Yield 57%, yellowish fine crystalline powder. Mp 178–180 °C (from CH_3CN). ^{1}H NMR (400 MHz, DMSO-d_6), δ, ppm (*J*, Hz): 2.78 (3H, s, 7-CH_3); 3.39 (3H, s, CO_2CH_3); 3.82 (3H, s, CO_2CH_3); 7.20–7.26 (1H, m, thiophen-2-yl); 7.54–7.71 (5H, m, Ph); 7.79–7.84 (1H, m, thiophen-2-yl); 7.96–8.01 (1H, m, thiophen-2-yl). ^{13}C NMR (101 MHz, DMSO-d6), δ, ppm: 10.5; 52.57; 52.60; 113.3; 116.1; 117.7; 128.6; 128.9; 129.0; 129.9; 131.47; 131.53; 131.6; 136.1; 139.4; 152.2; 162.6; 163.8; 164.7. EI-MS (70 eV), *m/z* (Irel (%)): 408 $[M+1]^+$ (27), 407 $[M]^{+\cdot}$(100), 376 (21), 375 (49), 344 (26), 343 (23), 289 (13), 288 (30), 152 (16), 151 (12), 77 (12). Found, %: C 62.05; H 4.30; N 10.51. $C_{21}H_{17}N_3O_4S$. Calculated, %: C 61.90; H 4.21; N 10.31.

Dimethyl 4-(4-methoxyphenyl)-7-methyl-2-(thiophen-2-yl)pyrrolo[2,1-*f*][1,2,4]triazine-5,6-dicarboxylate (**16f**). Reaction conditions: 2.5 mL dry tetrahydrofuran, reaction time 4 days. Yield 57%, bright yellow powder. Mp 211–213 °C (from CH_3CN). ^{1}H NMR (400 MHz, DMSO-d_6), δ, ppm (*J*, Hz): 2.79 (3H, s, 7-CH_3); 3.52 (3H, s, CO_2CH_3); 3.83 (3H, s, CH_3); 3.88 (3H, s, CH_3); 7.10–7.18 (2H, m, 4-CH_3O-C_6H_4); 7.21–7.29 (1H, m, thiophen-2-yl); 7.65–7.74 (2H, m, 4-CH_3O-C_6H_4); 7.79–7.86 (1H, m, thiophen-2-yl); 7.97–8.04 (1H, m, thiophen-2-yl). ^{13}C NMR (101 MHz, DMSO-d_6), δ, ppm: 10.6; 52.6; 52.8; 56.0; 113.3; 114.4; 116.0; 117.6; 128.4; 129.0; 129.7; 130.6; 131.3; 131.4; 139.6; 152.1, 161.9; 162.4; 163.9; 164.9. EI-MS (70 eV), *m/z* (Irel (%)): 438 $[M+1]^+$ (26), 437 $[M]^{+\cdot}$(100), 406 (13), 405 (26), 374 (35), 373 (36), 318 (21), 317 (15), 139 (10). Found, %: C 60.48; H 4.36; N 9.71. $C_{22}H_{19}N_3O_5S$. Calculated, %: C 60.40; H 4.38; N 9.61.

Dimethyl 7-methyl-4-(naphthalen-2-yl)-2-(thiophen-2-yl)pyrrolo[2,1-*f*][1,2,4]triazine-5,6-dicarboxylate (**16g**). Reaction conditions: 3.0 mL dry tetrahydrofuran, reaction time 3 days. Yield 52%, orange-colored fine crystalline powder. Mp 170–171 °C. ^{1}H NMR (400 MHz, DMSO-d_6), δ, ppm (*J*, Hz): 2.80 (3H, s, 7-CH_3); 3.25 (3H, s, CO_2CH_3); 3.82 (3H, s, CO_2CH_3); 7.21–7.29 (1H, m, thiophen-2-yl); 7.61–7.72 (2H, m, naphthalen-2-yl); 7.78–7.88 (2H, m, naphthalen-2-yl (1H), thiophen-2-yl (1H)); 7.99–8.08 (3H, m, naphthalen-2-yl (2H), thiophen-2-yl (1H)); 8.08–8.15 (1H, m, naphthalen-2-yl); 8.26 (1H, br s, naphthalen-2-yl). ^{13}C NMR (101 MHz, *DMSO-d6*), δ, ppm: 10.6; 52.57; 52.61; 113.4; 116.3; 117.9; 125.5; 128.0; 128.3; 128.4; 128.8; 129.0; 129.05; 129.14; 130.0; 131.5; 131.6; 132.4; 133.4; 134.5; 139.4; 152.2; 162.5; 163.8; 164.8. EI-MS (70 eV), *m/z* (Irel (%)): 458 $[M+1]^+$ (30), 457 $[M]^+$ (100), 394 (39), 393 (55), 338 (17), 337 (21), 229 (13), 200 (12), 127 (13). Found, %: C 65.51; H 4.14; N 9.16. $C_{25}H_{19}N_3O_4S$. Calculated, %: C 65.63; H 4.19; N 9.18.

Dimethyl 7-methyl-2,4-di(thiophen-2-yl)pyrrolo[2,1-*f*][1,2,4]triazine-5,6-dicarboxylate (**16h**). Reaction conditions: 2.0 mL dry tetrahydrofuran, reaction time 4 days. Yield 37%, yellow powder. Mp 152–153 °C (from EtOH). ^{1}H NMR (600 MHz, DMSO-d_6), δ, ppm (*J*,

Hz): 2.84 (3H, s, 7-CH_3); 3.70 (3H, s, CO_2CH_3); 3.88 (3H, s, CO_2CH_3); 7.20–7.25 (1H, m, thiophen-2-yl); 7.25–7.30 (1H, m, thiophen-2-yl); 7.55–7.60 (1H, m, thiophen-2-yl); 7.70–7.75 (1H, m, thiophen-2-yl); 7.95–8.00 (2H, m, thiophen-2-yl). ^{13}C NMR (101 MHz, DMSO-d_6), δ, ppm: 10.7; 52.6; 53.1; 113.2; 116.1; 116.2; 128.9; 129.6; 131.4; 131.5; 132.0; 133.7; 138.8; 139.1; 151.6; 155.1; 163.7; 165.5. EI-MS (70 eV), *m/z* (Irel (%)): 414 $[M+1]^+$ (24), 413 $[M]^+$ (26), 382 (31), 381 (70), 323 (28), 295 (27), 158 (30). Found, %: C, 55.25; H, 3.70; N, 10.41. $C_{19}H_{15}N_3O_4S_2$. Calculated, %: C 55.19; H 3.66; N 10.16.

Dimethyl 2-(4-chlorophenyl)-7-methyl-4-phenylpyrrolo[2,1-*f*][1,2,4]triazine-5,6-dicarboxylate (**17a**). Reaction conditions: 2.0 mL dry tetrahydrofuran, reaction time 4 days. Yield 37%, light yellow powder. Mp 182–183 °C (from EtOH). ^{1}H NMR (400 MHz, DMSO-d_6), δ, ppm (*J*, Hz): 2.86 (3H, s, 7-CH_3); 3.42 (3H, s, CO_2CH_3); 3.85 (3H, s, CO_2CH_3); 7.57–7.69 (5H, m, 4-Cl-C_6H_4 (2H) и Ph (3H)); 7.71–7.77 (2H, m, 4-Cl-C_6H_4); 8.37–8.45 (2H, m, Ph). ^{13}C NMR (101 MHz, DMSO-d_6), t = 50 °C, δ, ppm:): 10.5; 52.47; 52.49; 113.0; 116.6; 117.8; 128.7; 128.8; 129.3; 129.5; 131.6; 131.7; 133.7; 136.35; 136.44; 153.7; 162.6; 163.8; 164.6. EI-MS (70 eV), *m/z* (Irel (%)): 437 $[M+2]^+$ (29), 436 $[M+1]^+$ (24), 435 $[M]^+$ (100), 405 (26), 404 (28), 403 (74), 3763 (23), 372 (38), 371 (39), 318 (25), 317 (32), 316 (51), 280 (28), 254 (34), 153 (38), 152 (99), 151 (80), 150 (52), 140 (40), 139 (53), 138 (48), 137 (44), 127 (40), 126 (85), 113 (30), 111 (42), 102 (58), 77 (81). Found, %: C, 63.21; H, 4.13; N, 9.51. $C_{23}H_{18}ClN_3O_4$. Calculated, %: C, 63.38; H, 4.16; N, 9.64.

2.2. Docking Studies

Molecular docking was carried out in ArgusLab 4.0.1 software [31] using the GADock genetic algorithm (elitism = 3) with the empirical scoring function AScore. Third-party molecules were removed from the complexes (with the exception of metal ions at binding sites), then the hydrogen atoms were added. Ligands for docking were prepared in DataWarrior 5.5.0 software [32] with generation of conformers (1 per structure) on MMFF94s+.

The size of binding sites is set automatically relative to the position of native ligands. To establish the quality of the modeling (the quality of reproduction of at least a reliably known position of the inhibitor), redocking of native ligands was carried out with the calculation of the root-mean-square deviation (RMSD), which does not exceed 2Å.

Two-dimensional maps of non-covalent interactions were prepared using the PoseEdit tool [33] from the ProteinsPlus web server (https://proteins.plus/, accessed on 1 September 2023) [34].

Three-dimensional overlays of the best docked positions were prepared using VMD 1.9.3 [35].

2.3. Viruses and Cells

Influenza virus A (strain A/Puerto Rico/8/34 (H1N1)), obtained from the collection of viruses of St. Petersburg Pasteur Institute (Saint Petersburg, Russia), was used in the experiments. Virus was propagated in the allantoic cavity of 10–12-day-old chicken embryos for 48 h at 36 °C and used for further in vitro study. MDCK cells (ATCC # CCL-34) were grown in 96-well plates in alpha minimum essential medium (alpha-MEM) (Biolot, St. Petersburg, Russia) with 10% fetal bovine serum (Biolot, St. Petersburg, Russia).

2.4. Cytotoxicity Assay

MDCK cells were seeded onto 96-well culture plates (104 cells per well) and incubated at 36 °C in 5% CO_2 until continuous monolayer formation. To assess the toxicity of compounds, a series of their three-fold dilutions at concentrations of 300 to 3.7 μg/mL in Eagle's MEM were prepared. The dilutions were added to the wells of the plates. Cells were incubated for 72 h at 36 °C under 5% CO_2. Further, cells were washed 2 times with saline (0.9% NaCl) and 100 μL/well of MTT solution (3-(4,5-dimethylthiazol-2-yl)-2,5-diphenyltetrazolium bromide) at a concentration of 0.5 mg/mL in MEM was added. The plates were incubated for 2 h at 36 °C, the liquid was removed and DMSO (0.1 mL per well)

was added. The optical density (OD) of the cells was measured on a Thermo Multiskan FC spectrophotometer (Thermo Fisher Scientific, Waltham, MA, USA) at a wavelength of 540 nm. Based on the obtained data, the CC_{50}, the concentration of the compound that destroys 50% of the cells in culture, was calculated for each specimen.

2.5. CPE Reduction Assay

The tested compounds in appropriate concentrations were added to MDCK cells (0.1 mL per well). MDCK cells were further infected with A/Puerto Rico/8/34 (H1N1) influenza virus (multiplicity of infection (MOI) 0.01). Plates were incubated for 72 h at 36 °C at 5% CO_2. After that, cell viability was assessed by the MTT test as described above. The cytoprotective activity of compounds was considered as their ability to increase the values of OD compared to control wells (with virus only, no drugs). Based on the results obtained, the values of IC_{50}, i.e., the concentration of compounds that results in protection of 50% of cells, were calculated using GraphPad Prism 10.0.2 software. Values of IC_{50} obtained in micrograms/mL were then translated into micromoles. Based on the obtained data, the selectivity index (SI), the ratio of CC_{50} to IC_{50}, was calculated for each compound.

2.6. Time-of-Addition Experiments

In order to determine the specific stage of the viral life cycle that is affected by the lead compound **15f**, MDCK cells previously seeded to 24-well plates were infected with influenza virus A/Puerto Rico/8/34 (H1N1) (m.o.i. 10) by adding the virus and further incubation for 1 h at 4 °C. Non-absorbed virions were removed by washing for 5 min with MEM. Cells were further incubated for 8 h at 36 °C at 5% CO_2. The time point when plates were transferred to 36 °C was referred to as zero. Compound **15f** (150 μg/mL) was added at the following time periods: (−2)–(−1) (before infecting); (−1)–0 (simultaneously to virion absorption); 0–2; 2–4; 4–6; 6–8 and (−2)–8 h. For each variant of the experiment, after incubation with compound, cells were washed for 5 min with MEM. After 8 h of growth, the level of virus reproduction (virus' titer) was determined in culture medium as described above.

3. Results and Discussion

3.1. Chemistry

It is known that N-alkylpyridinium and other azinium cations, especially those containing a CH_2W (W—an electron-withdrawing group) moiety at the quaternary nitrogen atom, are precursors of N-heterocyclic ylides capable of participating in various 1,3-DP CA reactions with both alkenes and acetylenes. A feature of 1,2,4-triazines is that the formation of ylides from N-alkyl-1,2,4-triazinium salts does not require the presence of electron-withdrawing groups in the N-alkyl moiety. The study of the reactivity of 1-alkyl-1,2,4-triazinium salts has shown that the deprotonation of 1-ethyl-3-alkylthio-5-aryl-1,2,4-triazinium salts in the presence of triethylamine leads to the formation of unstabilized azomethine ylides, which react in situ with dimethyl acetylenedicarboxylate to form pyrrolotriazines [36].

In this work, pyrrolo[2,1-*f*][1,2,4]triazines **14**–**17**, bearing aryl and thienyl substituents, have been synthesized through 1,3-dipolar cycloaddition of 3,5-disubstituted N(1)-ethyl-1,2,4-triazinium cations **10**–**13** with dimethyl acetylenedicarboxylate in the presence of triethylamine (Scheme 1).

The starting 3,5-disubstituted 1,2,4-triazines **6**–**9** were obtained by cyclization of the corresponding aryl(thienyl)amidrazones **1**–**4** with aryl(thienyl) glyoxals **5a**–**h** according to the modified procedures [28]. Then, the resulting 3,5-disubstituted 1,2,4-triazines **6**–**9** were treated with Meerwein's reagent to obtain N(1)-ethyl-1,2,4-triazinium salts **10**–**13**, which were isolated in crystalline form and recrystallized from absolute ethanol. Unstabilized ylides **A** were generated in situ from N(1)-1,2,4-triazinium salts **10**–**13** in absolute dioxane or tetrahydrofuran in the presence of triethylamine. Ylides **A** reacted with dimethyl acetylenedicarboxylate to form target pyrrolo[1,2-*f*][1,2,4]triazines **14**–**17** via the 1,3-DP CA.

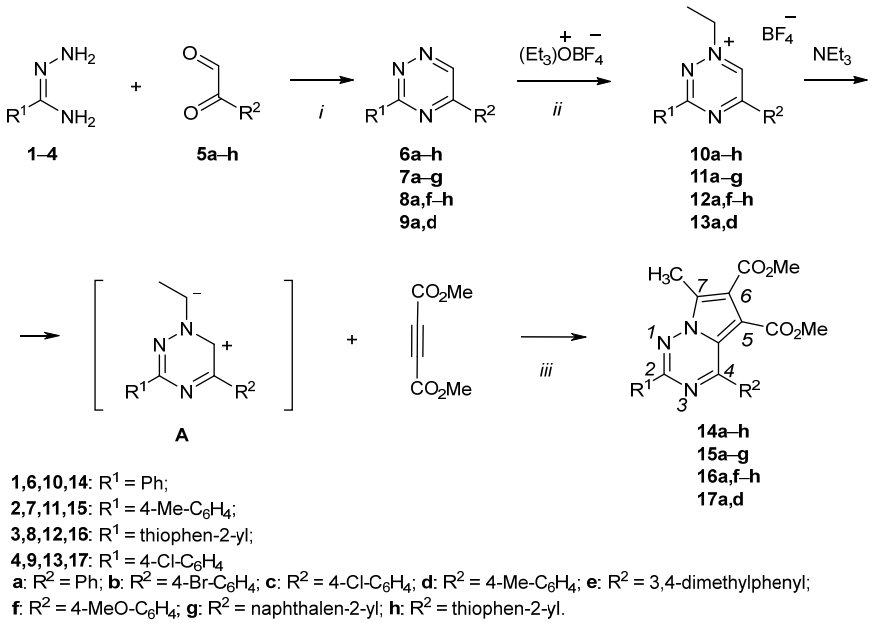

Scheme 1. Reaction conditions: (*i*) EtOH, 0–5 °C, 24–48 h; (*ii*) Et_3OBF_4, EDC, rt, 2–3 h; (*iii*) DMAD, NEt_3, THF (dioxane), rt, 2–4 days. Synthesis of pyrrolo[2,1-*f*][1,2,4]triazines **14c**, **15d**, **17d** has been described in the previous work [24].

Dimethyl 7-methyl-2-R^1-4-R^2-pyrrolo[2,1-*f*][1,2,4]triazine-5,6-dicarboxylates **14–17** were synthesized as yellow, bright yellow or orange substances, soluble in dimethyl sulfoxide, dioxane, hot acetonitrile and ethanol and practically insoluble in water. The structures of the obtained compounds **14–17** were confirmed by ^{1}H and ^{13}C NMR, mass spectra and elemental analysis. The ^{1}H NMR spectra show the characteristic proton signals of 7-methyl moiety at δ 2.78–2.89 ppm and two carbomethoxy moieties at δ 3.27–3.70 and 3.82–3.89 ppm. The ^{13}C NMR spectra contain the corresponding carbon nuclei signals of two carbonyl groups at δ 163.71–163.97 and 164.64–165.59 ppm, as well as pyrrolo[2,1-*f*][1,2,4]triazine core: triazine ring C(2) at δ 155.13–162.63, C(4) at δ 151.57–154.71 and pyrrole cycle C(5) coupled with it, C(6) and C(7) in the region of δ 112.38–118.03 ppm.

3.2. Antiviral and Cytotoxicity Studies

The results of in vitro studies of cytotoxic and antiviral activity of compounds **14–17** against influenza virus strain A/Puerto Rico/8/34 (H1N1) on MDCK cell culture are summarized in Table 1.

Based on the results of in vitro studies, it has been shown that, in general, all compounds are characterized by low toxicity, but a structure–toxicity relationship has been revealed. The highest toxicity has been found for compound **14h** (CC_{50} = 106 ± 8 μM) with a phenyl moiety at position 2 and thienyl moiety at position 4 of the pyrrolo[2,1-*f*][1,2,4]triazine scaffold. At the same time, compound **16a**, in which the phenyl and thienyl moieties are swapped compared to **14h**, has been found to have 5 times lower toxicity (CC_{50} = 616 ± 28 μM). However, a similar pattern has not been observed for isomers **14d** and **15a**, which differ in the position of the phenyl and *p*-tolyl moieties.

Dimethyl 7-methyl-2-R^1-4-R^2-pyrrolo[2,1-*f*][1,2,4]triazine-5,6-dicarboxylates **14–17** showed different abilities to inhibit the reproduction of influenza A/Puerto Rico/8/34 (H1N1) virus.

2-Phenyl-substituted 4-R^2-pyrrolo[2,1-*f*][1,2,4]triazines **14a,b,d–h** were shown to have the least inhibitory activity compared to other studied compounds. Only compound **14g** (R^2 = naphthalene-2-yl) demonstrated IC_{50} of 188 ± 22 μg/mL (SI = 4).

Table 1. Cytotoxic and antiviral properties of pyrrolo[2,1-*f*][1,2,4]triazines **14**–**17**.

Structure		R^2	CC_{50}, μg/mL	IC_{50}, μg/mL	SI
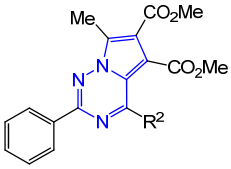	**14a**	Ph	>747	>747	1
	14b	4-Br-C_6H_4	>625	523 ± 61	1
	14d	4-Me-C_6H_4	665 ± 34	>229	3
	14e	3,4-dimethylphenyl	>722	>722	1
	14f	4-OMe-C_6H_4	>699	>699	1
	14g	naphthalen-2-yl	>695	188 ± 22	4
	14h	thien-2-yl	106 ± 8	>73	1
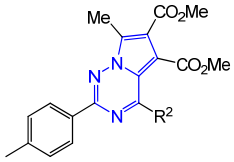	**15a**	Ph	>722	93 ± 14	8
	15b	4-Br-C_6H_4	>300	55	5
	15c *	4-Cl-C_6H_4	>667	58 ± 7	12
	15e *	3,4-dimethylphenyl	>676	69 ± 8	10
	15f *	4-OMe-C_6H_4	>673	4 ± 1	188
	15g	naphthalen-2-yl	121 ± 7	>71	2
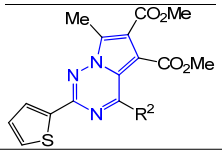	**16a**	Ph	616 ± 28	>245	3
	16f *	4-OMe-C_6H_4	>229	23 ± 3	10
	16g	naphthalen-2-yl	>656	107 ± 11	6
	16h *	thien-2-yl	>726	15 ± 3	48
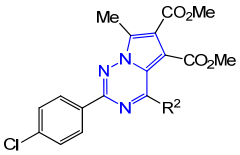	**17a** *	Ph	>688	66 ± 8	10
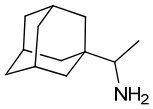	Rimantadine		62	12	5
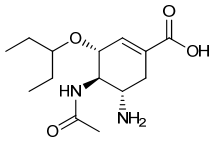	Oseltamivir carboxylate		>200	0.26 ± 0.04	>769
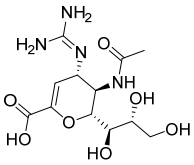	Zanamivir		>100	0.29 ± 0.05	>345

* Objects with good selectivity index (SI ≥ 10).

Replacing the phenyl moiety with *p*-tolyl at C-2 of the pyrrolotriazine heterocycles resulted in a better inhibition of the influenza virus. Thus, 2-*p*-tolyl-4-R^2-pyrrolo[2,1-*f*][1,2,4]triazines containing unsubstituted phenyl moiety at C-4 (**15a**), as well as 4-chloro- and 3,4-dimethylsubstituted phenyl groups (**15c** and **15e**), showed inhibitory activity in the range of 58–93 μg/mL (SI = 8–12). The lead compound in antiviral assay with low cytotoxicity (CC_{50} > 673 μg/mL) is pyrrolotriazine **15f**, containing a 4-methoxyphenyl moiety at position 4 (IC_{50} = 4 ± 1 μg/mL; SI = 188). It is noteworthy that 4-(4-methoxyphenyl)pyrrolotriazine **14f**, containing a phenyl moiety at position 2, did not exhibit antiviral activity at all (IC_{50} > 699 μg/mL; SI = 1).

In the series of 2-thiophen-2-yl-4-R^2-pyrrolo[2,1-*f*][1,2,4]triazines, the best inhibitory activity was shown by pyrrolotriazines **16f** and **16h**, containing at the C-4 atom *p*-methoxyphenyl

(CC_{50} > 229 μM, IC_{50} = 23 ± 3 μM, SI = 10) and thienyl (CC_{50} > 726 μM, IC_{50} = 15 ± 3 μM, SI = 48) moieties, respectively.

The pyrrolo[2,1-*f*][1,2,4]triazine **17a** (4-Cl-phenyl at C-2 and phenyl at C-4 pyrrolotriazine ring) showed antiviral activity at a concentration of IC_{50} = 66 ± 8 μM (SI = 10). Previously, the pyrrolotriazine **14c**, characterized by the different substitution pattern (phenyl at C-2 and 4-Cl-phenyl at C-4 pyrrolotriazine ring), demonstrated the high inhibitory activity (IC_{50} = 2.5 ± 0.2 μM, SI = 40) against influenza virus A/Puerto Rico/8/34 (H1N1) with relatively low cytotoxicity CC_{50} > 100 ± 7 μM (Figure 2).

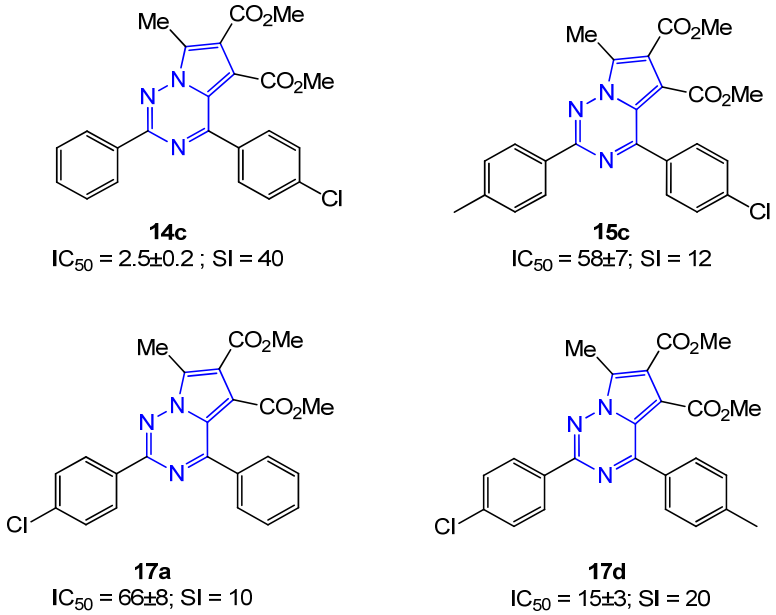

Figure 2. Inhibitory activity of pyrrolo[2,1-*f*][1,2,4]triazines containing a 4-Cl-phenyl moiety against A/Puerto Rico/8/34 (H1N1) virus strain (antiviral activity of **14c** and **17d** was described previously [24]).

Pyrrolo[2,1-*f*][1,2,4]triazine **15c**, containing *p*-tolyl and 4-Cl-phenyl moieties at positions 2 and 4, respectively, showed similar antiviral activity to pyrrolo[2,1-*f*][1,2,4]triazine **17d** with the opposite arrangement of moieties at C-2 and C-4 positions (Figure 2).

An analysis of the obtained data led us to controversial SAR, as there was no clear correlation between antiviral activity and the nature of aryl/thienyl moieties and their position on the pyrrolo[2,1-*f*][1,2,4]triazine core. Apparently, the main contribution to the ability to suppress virus reproduction is made by the core structure, pyrrolo[2,1-*f*][1,2,4]triazine, and the issue of its functionalization requires further study.

3.3. Molecular Docking Studies

To establish a plausible mechanism of antiviral activity, molecular docking for structures of obtained compounds was carried out on four key influenza proteins: (1) hemagglutinin—a surface protein responsible for attachment to the host cell and membrane fusion. Two binding sites were suggested for docking: the F0045(S)-binding site (FBS) involved in the process of membrane fusion (PDB ID: 6wcr) [37] and the receptor-binding site (RBS) [38]; (2) neuraminidase (NA)—a surface protein responsible for the sialic acid cleavage from cell surface and progeny virions facilitating virus release from infected cells (PDB ID: 3ti5); (3) PA—a protein containing the endonuclease domain of RNA-dependent RNA polymerase that cleaves host mRNA to prime viral mRNA transcription (PDB ID: 4yyl); (4) PB2—a protein containing the cap-binding domain of RNA-dependent RNA polymerase (PDB ID: 5jun). For the NA and PB2 proteins from the corresponding complexes, their overall similarity to the same proteins of the H1N1/Puerto Rico/8/34 viral strain (Table 2) and similarity to their binding sites were calculated.

Table 2. Characteristics of the target protein–ligand complexes used.

Target	FBS	RBS	PA	NA	PB2
PDB	**6wcr**		**4yyl**	**3ti5**	**5jun**
Viral strain	H1N1/Puerto Rico/8/34			H1N1/California/ 04/2009	H3N2/Beijing/ 39/1975
Sequence similarity to A/Puerto Rico/8/34	-	-	-	86%	93%
Binding site similarity to A/Puerto Rico/8/34	-	-	-	100%	100%

6wcr, 4yyl, 3ti5, 5jun – PDB IDs from Protein Data Bank (https://www.rcsb.org/, accessed on 31 August 2023).

Protein–ligand complexes with known inhibitors (Figure 3) were downloaded from the RCSB database: hemagglutinin (pdb: 6wcr) and endonuclease (pdb:4yyl) complexes with inhibitors are presented for the virus strain H1N1/Puerto Rico/8/34, and complexes of neuraminidase (pdb:3ti5) and PB2 protein (pdb:5jun) for other viral strains.

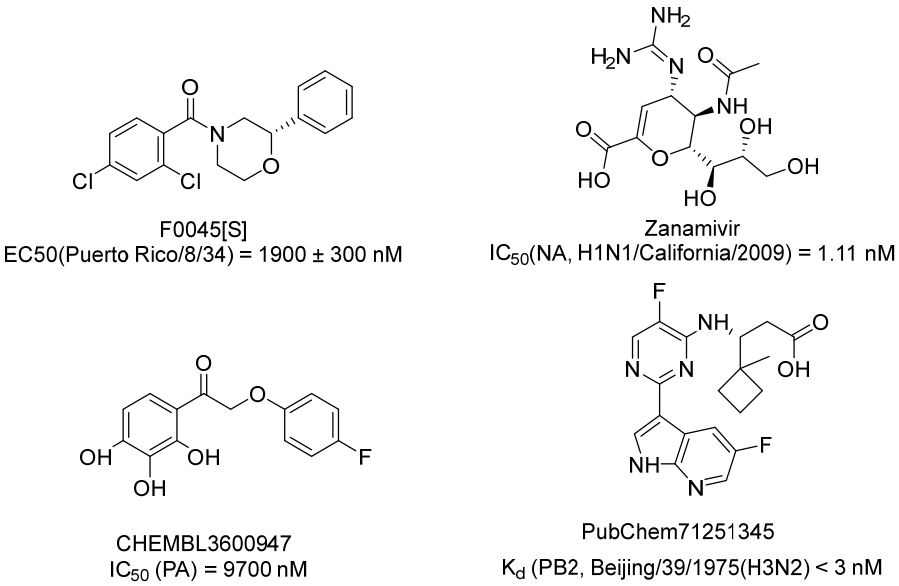

Figure 3. Structures of native ligands from protein–ligand complexes: inhibitor of hemagglutinin (F0045(S)), neuraminidase (zanamivir), PA (CHEMBL3600947), PB2 (PubChem71251345).

The results of molecular docking are shown in Table 3.

The obtained quantitative docking score values have indicated the theoretical possibility of the formation of complexes of the studied ligands **14**–**17** with the selected targets. Based on the results of in silico and in vitro studies, the Pearson correlation coefficient was calculated between the docking score for each target and the experimental IC_{50} value including obtained data for zanamivir and oseltamivir carboxylate. Direct in silico–in vitro correlation is observed for the calculated data for neuraminidase (Pearson correlation coefficient 0.47) and hemagglutinin receptor site RBS (Pearson correlation coefficient 0.40). For other targets, the correlation is either inverse or absent. Thus, the correlation coefficients between the obtained results of docking and primary biological tests have demonstrated that the most likely target is neuraminidase among the four proposed target proteins.

Table 3. Results of molecular docking and in vitro studies of antiviral pyrazolo[2,1-*f*][1,2,4]triazines.

Compound	Docking Score, kcal/mol					IC_{50}, μg/mL
	FBS 6wcr	**RBS 6wcr**	**NA 3ti5**	**PA 4yyl**	**PB2 5jun**	
F0045[S]	−8.34 (1.61Å)	–	-	-	-	-
Zanamivir	-	-	−10.79 (1.01 Å)	-	-	0.29
CHEMBL3600947	-	-	-	−8.22 (1.81 Å)	-	-
PubChem71251345	-	-	-	-	−11.66 (1.35 Å)	-
Oseltamivir carboxylate			−10.10			0.26
14a	−7.04	−7.73	−6.46	−9.57	−10.97	>747
14b	−8.42	−7.27	−7.09	−9.90	−12.00	523 ± 61
14c	−9.45	−8.30	−7.08	−8.82	−11.98	2.5 [24]
14d	−8.46	−8.39	−9.14	−10.35	−11.37	>229
14e	−8.71	−7.99	−7.70	−10.40	−9.92	>722
14f	−7.93	−7.74	−8.40	−9.84	−12.21	>699
14g	−8.13	−7.50	−7.64	−10.34	−13.19	188 ± 22
14h	−8.55	−7.64	−8.00	−10.43	−10.89	>73
15a	−8.37	−6.90	−9.72	−9.74	−10.48	93 ± 14
15b	−7.68	−8.80	−7.43	−9.70	−13.04	55
15c	−8.26	−7.86	−8.72	−9.83	−10.45	58 ± 7
15d	−8.96	−8.57	−8.98	−10.99	−11.14	25 [24]
15e	−7.68	−7.07	−8.69	−8.27	−12.74	69 ± 8
15f	−7.00	−7.95	−8.25	−9.13	−10.34	4 ± 1
15g	−10.06	−7.39	−8.53	−11.02	−10.34	>71
16a	−8.00	−8.47	−6.42	−10.08	−11.81	>245
16f	−8.82	−8.30	−8.73	−8.71	−10.04	23 ± 3
16g	−9.95	−9.29	−7.97	−10.44	−10.96	107 ± 11
16h	−8.05	−8.33	−8.32	−8.50	−10.48	15 ± 3
17a	−8.97	−7.85	−9.23	−9.28	−9.82	66 ± 8
17d	−7.93	−8.33	−9.39	−9.49	−13.67	15 [24]
Pearson test: docking score—IC_{50}	−0.07	0.40	0.47	−0.30	−0.20	

3.4. Time-of-Addition Test

A more detailed biological study was performed to assess the inhibition of the viral cycle stage by the lead compound in a time-of-addition experiment. Herein, compound **15f** was added to the infected cell culture at different time points after infection and the yield of virus progeny was assessed. The results are summarized in Figure 4.

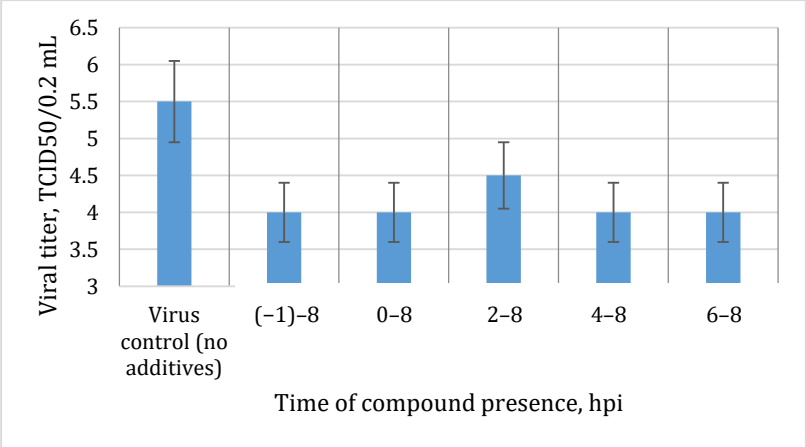

Figure 4. Infectious activity of influenza A/Puerto Rico/8/34 (H1N1) virus in the presence of compound **15f** depending on the time of addition.

It is known that the life cycle of the influenza virus (the time from adsorption of the virus on the plasma membrane to the release of the first generation of viral progeny) takes about 8 h. As can be seen from the data presented in Figure 4, the activity of the compound is maintained until the late stages of the cycle, which suggests that the target of action of compound **15f** is a protein required in these stages of the viral cycle. One of these proteins is viral neuraminidase, which cleaves progeny virions from the cell surface. Thus, according to the consistent results of previous in silico and in vitro studies, neuraminidase has been proposed as a possible target for the antiviral activity of compound **15f** and the series of pyrrolo[2,1-*f*][1,2,4]triazines.

3.5. Possible SAR and Ligand–Target Interactions

The binding modes of the ligands into the active site of neuraminidase were also assessed to establish key non-covalent interactions with the suggested target. Compounds with different chemical environments and IC_{50} values were selected for the analysis: **15f** (IC_{50} = 4 ± 1 μg/mL); **14f** (IC_{50} > 699 μg/mL); **16f** (IC_{50} = 23 ± 3 μg/mL); **16h** (IC_{50} = 15 ± 3 μg/mL) (Figure 5A–D).

Figure 5F shows that the general pattern for the active compounds is the proximity of the pyrrolotriazine ring in the plane of the dihydropyran ring of zanamivir (Figure 5E,F). The influence of substituents at the 2 and 4 positions of pyrrolo[2,1-*f*][1,2,4]triazine ring on the IC_{50} remains questionable.

Analysis of the structure–activity relationship for the set of compounds without docking studies (Table 1) allows us to make a preliminary conclusion about the preferential presence of an unsubstituted aromatic moiety at position 2 and an aromatic moiety with a hydrogen bond acceptor at position 4 of the pyrrolo[2,1-*f*][1,2,4]triazine core.

However, the results of docking for compounds **16f**, **16h** (Figure 5C,D) indicate the optional nature of the proposed interactions: **16h** is oriented due to hydrophobic interactions with thienyl moieties at positions 2 and 4 of pyrrolo[2,1-*f*][1,2,4]triazine without forming additional hydrogen bonds with them; **16f** is oriented, among other things, due to the formation of a hydrogen bond and stacking interaction with the thienyl moiety at position 2 without additional hydrophobic interactions.

Some disagreements in the structure–activity relationship may be caused by either unaccounted binding modes of the ligands into the suggested target protein or by another competitive mechanism of action.

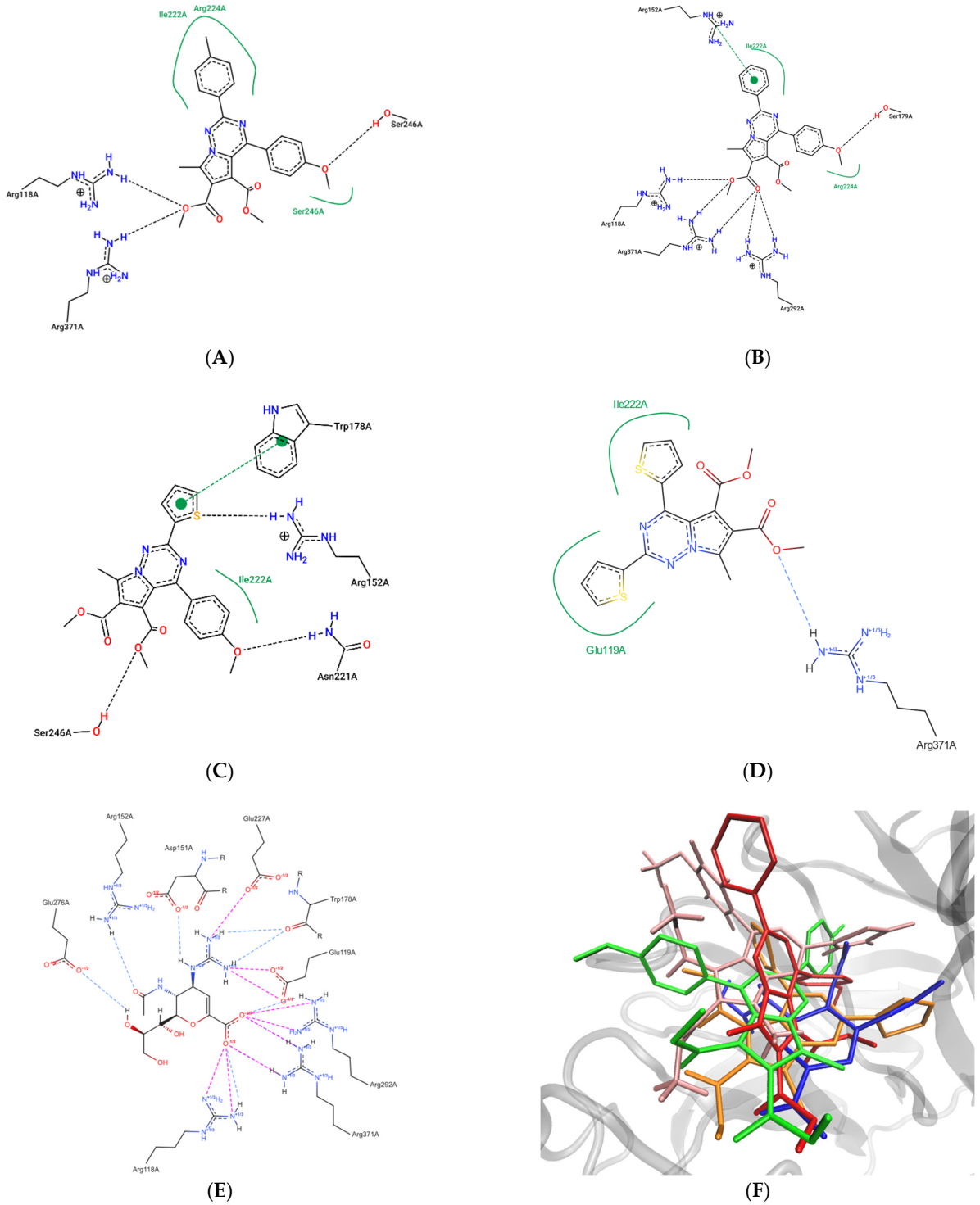

Figure 5. The results of docking of several ligands into neuraminidase active site: (**A**)—2D map of non-covalent interactions of docked **15f**; (**B**)—2D map of non-covalent interactions of docked **14f**; (**C**)—2D map of non-covalent interactions of docked **16f**; (**D**)—2D map of non-covalent interactions of docked **16h**; (**E**)—2D map of non-covalent interactions of native ligand (zanamivir); (**F**)—overlay of the best docked positions of the ligands against native position of zanamivir: **15f** (green); **14f** (red); **16f** (pink); **16h** (orange); zanamivir (blue).

4. Conclusions

In summary, a number of novel 2,4-(het)aryl derivatives of substituted pyrrolo[2,1-*f*][1,2,4]triazines have been synthesized by reacting N(1)-ethyl-1,2,4-triazinium tetrafluo-

roborates with dimethyl acetylenedicarboxylate. In vitro experiments, performed for the compounds of this series, have revealed a low cytotoxicity and a high antiviral activity against influenza virus strain A/Puerto Rico/8/34 (H1N1). Based on the results of molecular docking and subsequent in-depth biological study, it has been established that inhibition of viral activity by the hit compound **15f** does occur at the later stages of the viral cycle, presumably because of interacting with neuraminidase. In order to reveal the "structure–antiviral activity" relationships entirely, the series of pyrrolo[2,1-*f*][1,2,4]triazines needs to be extended, as well as additional in silico studies using molecular dynamics and in vitro studies on inhibition of the enzymatic activity of the suggested protein target are to be carried out within the framework of our next works.

Supplementary Materials: The following supporting information can be downloaded at: https://www.mdpi.com/article/10.3390/chemistry5040171/s1, NMR data of the synthesized novel 3,5-disubstituted 1,2,4-triazines, 1,2,4-triazin-1-ium tetrafluoroborates and pyrrolo[2,1-*f*][1,2,4]triazines. Figures S1–S5: ^{1}H NMR spectra of 3,5-disubstituted 1,2,4-triazines **6e**, **6h**, **7e**, **7f**, **8h**. Figures S6–S21: ^{1}H NMR spectra of 1,2,4-triazin-1-ium tetrafluoroborate **10**–**13**. Figures S22–S39: ^{1}H and ^{13}C NMR spectra of 7-methyl-5,6-dialkoxycarbonyl-2-R^{2}-4-R^{1}-pyrrolo[2,1-*f*][1,2,4]triazines **14**–**17**.

Author Contributions: Author Contributions: Conceptualization, V.N.C., V.L.R. and V.V.Z.; methodology, N.N.M., S.K.K., I.I.B. and V.V.Z.; software, I.I.B.; validation, V.L.R. and V.V.Z.; formal analysis, V.N.C.; investigation, N.N.M., I.I.B., Y.L.E., A.V.S. and P.A.I.; resources, V.L.R. and V.V.Z.; data curation, S.K.K. and V.V.Z.; writing—original draft preparation, N.N.M., I.I.B., Y.L.E., A.V.S. and P.A.I.; writing—review and editing, S.K.K.; visualization, N.N.M., I.I.B. and V.V.Z.; supervision, M.V.V.; project administration, M.V.V., S.K.K. and V.V.Z.; funding acquisition, V.L.R. and V.V.Z. All authors have read and agreed to the published version of the manuscript.

Funding: This research was supported by the Ministry of Science and Higher Education of the Russian Federation: Agreement on granting grants from the federal budget in the form of subsidies in accordance with paragraph 4 of Article 78.1 of the Budget Code of the Russian Federation (Moscow, October 1, 2020, No. 075-15-2020-777).

Data Availability Statement: Data are contained within the article or Supplementary Materials.

Conflicts of Interest: The authors declare no conflict of interest.

References

1. Adlhoch, C.; Fusaro, A.; Gonzales, J.L.; Kuiken, T.; Melidou, A.; Mirinavičiūtė, G.; Niqueux, É.; Ståhl, K.; Staubach, C.; Terregino, C.; et al. Scientific report: Avian influenza overview April–June 2023. *EFSA J.* **2023**, *21*, e08191.
2. Paget, J.; Danielle Iuliano, A.; Taylor, R.J.; Simonsen, L.; Viboud, C.; Spreeuwenberg, P. Estimates of Mortality Associated with Seasonal Influenza for the European Union from the GLaMOR Project. *Vaccine* **2022**, *40*, 1361–1369. [CrossRef]
3. Chakraborty, S.; Ashwini, C. Fighting the flu: A brief review on anti-influenza agents. *Biotechnol. Genet. Eng. Rev.* **2023**, 1–52. [CrossRef]
4. Wang, J.; Sun, Y.; Liu, S. Emerging antiviral therapies and drugs for the treatment of influenza. *Expert Opin. Emerg. Drugs* **2022**, *27*, 389–403. [CrossRef]
5. Kiselev, O.I. *Chemotherapy and Influenza Chemotherapy (Eng. Tansl.)*; LLC "Rostok": Saint Petersburg, Russia, 2011; 272p, ISBN 978-5-94668-101-8.
6. Tsvetkov, V.V.; Golobkov, G.S. Neuraminidase inhibitors are the gold standard for antiviral therapy of influenza type A. *Med. Counc.* **2017**, *4*, 25–30.
7. Król, E.; Rychłowska, M.; Szewczyk, B. Antivirals—Current trends in fighting influenza. *Acta Biochim. Pol.* **2014**, *61*, 495–504. [CrossRef]
8. Javanian, M.; Barary, M.; Ghebrehewet, S.; Koppolu, V.; Vasigala, V.; Ebrahimpour, S. A brief review of influenza virus infection. *J. Med. Virol.* **2021**, *93*, 4638–4646. [CrossRef]
9. Lampejo, T. Influenza and antiviral resistance: An overview. *Eur. J. Clin. Microbiol. Infect. Dis.* **2020**, *39*, 1201–1208. [CrossRef]
10. Yoshino, R.; Yasuo, N.; Sekijima, M. Molecular dynamics simulation reveals the mechanism by which the influenza cap-dependent endonuclease acquires resistance against baloxavir marboxil. *Sci. Rep.* **2019**, *9*, 17464. [CrossRef]
11. Sato, M.; Takashita, E.; Katayose, M.; Nemoto, K.; Sakai, N.; Fujisaki, S.; Hashimoto, K.; Hosoya, M. Detection of variants with reduced baloxavir marboxil and oseltamivir susceptibility in children with influenza A during the 2019–2020 influenza season. *J. Infect. Dis.* **2021**, *224*, 1735–1741. [CrossRef]
12. Amorim, M.J.; Kao, R.Y.; Digard, P. Nucleozin targets cytoplasmic trafficking of viral ribonucleoprotein-Rab11 complexes in influenza A virus infection. *J. Virol.* **2013**, *87*, 4694–4703. [CrossRef]

13. Liu, T.; Liu, M.; Chen, F.; Chen, F.; Tian, Y.; Huang, Q.; Liu, S.; Yang, J. A Small-Molecule Compound Has Anti-influenza A Virus Activity by Acting as a "PB2 Inhibitor". *Mol. Pharm.* **2018**, *15*, 4110–4120. [CrossRef]
14. Mifsud, E.J.; Hayden, F.G.; Hurt, A.C. Antivirals Targeting the Polymerase Complex of Influenza Viruses. *Antivir. Res.* **2019**, *169*, 104545. [CrossRef]
15. Basu, A.; Komazin-Meredith, G.; McCarthy, C.; Antanasijevic, A.; Cardinale, S.C.; Mishra, R.K.; Barnard, D.L.; Caffrey, M.; Rong, L.; Bowlin, T.L. Molecular Mechanism Underlying the Action of Influenza A Virus Fusion Inhibitor MBX2546. *ACS Infect. Dis.* **2017**, *3*, 330–335. [CrossRef]
16. Chen, Z.; Cui, Q.; Caffrey, M.; Rong, L.; Du, R. Small molecule inhibitors of influenza virus entry. *Pharmaceuticals* **2021**, *14*, 587. [CrossRef]
17. Shen, X.; Zhang, X.; Liu, S. Novel hemagglutinin-based influenza virus inhibitors. *J. Thorac. Dis.* **2013**, *5*, S149–S159.
18. Yang, J.; Li, M.; Shen, X.; Liu, S. Influenza A virus entry inhibitors targeting the hemagglutinin. *Viruses* **2013**, *5*, 352–373. [CrossRef]
19. Ott, G.R.; Favor, D.A. Pyrrolotriazines: From C-nucleoside stokinases and back again, the remark able journey of a versatilenitrogenheterocycle. *Bioorg. Med. Chem. Lett.* **2017**, *27*, 4238–4246. [CrossRef]
20. Li, Q.; Groaz, E.; Rocha-Pereira, J.; Neyts, J.; Herdewijn, P. Anti-norovirus activity of C7-modified 4-amino-pyrrolo[2,1-*f*][1,2,4]triazine C-nucleosides. *Eur. J. Med. Chem.* **2020**, *195*, 112198. [CrossRef]
21. Clarke, M.O.; Mackman, R.; Byun, D.; Hui, H.; Barauskas, O.; Birkus, G.; Chun, B.-K.; Doerffler, E.; Feng, J.; Karki, K.; et al. Discovery of β-d-2′-deoxy-2′-α-*f*luoro-4′-α-cyano-5-aza-7,9-dideaza adenosine as a potent nucleoside inhibitor of respiratory syncytial virus with excellent selectivity over mitochondrial RNA and DNA polymerases. *J. Med. Chem. Lett.* **2015**, *25*, 2484–2487. [CrossRef]
22. Mackman, R.L.; Parrish, J.P.; Ray, A.S.; Theodore, D.A. Methods and Compounds for Treating Paramyxoviridae Virus Infections. Patent WO 2012012776, 26 January 2012.
23. Chupakhin, O.N.; Rusinov, V.L.; Varaksin, M.V.; Ulomskiy, E.N.; Savateev, K.V.; Butorin, I.I.; Du, W.; Sun, Z.; Charushin, V.N. Triazavirin—A Novel Effective Antiviral Drug. *Int. J. Mol. Sci.* **2022**, *23*, 14537. [CrossRef]
24. Mochulskaya, N.N.; Kotovskaya, S.K.; Rusinov, V.L.; Charushin, V.N.; Zarubaev, V.V.; Volobueva, A.S. Dimethyl 7-methyl-2-(pyrrolidine-1-yl)-4-phenylpyrrolo[2,1-*f*][1,2,4]triazine-5,6-dicarboxylate and Dimethyl 7-methyl-2-(4-R1-phenyl)-4-(4-R2-phenyl)pyrrolo[2,1-*f*][1,2,4]triazine-5,6-dicarboxylates Exhibiting Antiviral Activity. Patent RU2790375 C1, 17 February 2023.
25. Akritopoulou-Zanze, I.; Wang, Y.; Zhao, H.; Djuric, S.W. Synthesis of Substituted Fused Pyridines, Pyrazines and Pyrimidines by Sequential Ugi/Inverse Electron Demand Diels–Alder Transformations. *Tetrahedron Lett.* **2009**, *50*, 5773–5776. [CrossRef]
26. Marchand, N.J.; Grée, D.M.; Martelli, J.T.; Grée, R.L.; Toupet, L.J. Synthesis and Reactivity of Cross-Conjugated Polyenones with a Planar Chirality. *J. Org. Chem.* **1996**, *61*, 5063–5072. [CrossRef]
27. Reid, C.M.; Ebikeme, C.; Barrett, M.P.; Patzewitz, E.-M.; Müller, S.; Robins, D.J.; Sutherland, A. Synthesis and Anti-Protozoal Activity of C2-Substituted Polyazamacrocycles. *Bioorg. Med. Chem. Lett.* **2008**, *18*, 2455–2458. [CrossRef]
28. O'Rourke, M.; Lang, S.A., Jr.; Cohen, E. 3-Aryl-as-triazines as potential antiinflammatory agents. *J. Med. Chem.* **1977**, *20*, 723–726. [CrossRef]
29. Wang, J.; Tang, D.; Li, Z.M.; Wu, P.; Meng, X.; Liu, Y.F.; Lu, G.Q.; Chen, B.H. Metal-Free Synthesis of 1,2,4-Triazines via a Coupled Domino Process in One-Pot. *Curr. Org. Chem.* **2017**, *21*, 183–188. [CrossRef]
30. Tang, D.; Wang, J.; Wu, P.; Guo, X.; Li, J.H.; Yang, S.; Chen, B.H. Synthesis of 1, 2, 4-triazine derivatives via [4+2] domino annulation reactions in one pot. *RSC Adv.* **2016**, *6*, 12514–12518. [CrossRef]
31. Thompson, M.A. *Arguslab, Version 4.0.1*; Planaria Software LLC: Seattle, WA, USA, 2004.
32. Sander, T.; Freyss, J.; von Korff, M.; Rufener, C. DataWarrior: An Open-Source Program For Chemistry Aware Data Visualization And Analysis. *J. Chem. Inf. Model* **2015**, *55*, 460–473. [CrossRef]
33. Diedrich, K.; Krause, B.; Berg, O.; Rarey, M. PoseEdit: Enhanced Ligand Binding Mode Communication by Interactive 2D Diagrams. *J. Comput. Aided Mol. Des.* **2023**, *37*, 491–503. [CrossRef]
34. Schöning-Stierand, K.; Diedrich, K.; Ehrt, C.; Flachsenberg, F.; Graef, J.; Sieg, J.; Penner, P.; Poppinga, M.; Ungethüm, A.; Rarey, M. ProteinsPlus: A Comprehensive Collection of Web-Based Molecular Modeling Tools. *Nucleic Acids Res.* **2022**, *50*, W611–W615. [CrossRef]
35. Humphrey, W.; Dalke, A.; Schulten, K. VMD: Visual Molecular Dynamics. *J. Mol. Graph.* **1996**, *14*, 33–38. [CrossRef]
36. Chupakhin, O.N.; Rudakov, B.V.; Alexeev, S.G.; Shorshnev, S.V.; Charushin, V.N. 1-Alkyl-1,2,4-Triazinium Ylides as 1,3-Dipoles in a Cycloaddition Reaction with Diethyl Acetylenedicarboxylate. *Mendeleev Commun.* **1992**, *2*, 85–86. [CrossRef]
37. Yao, Y.; Kadam, R.U.; Lee, C.-C.D.; Woehl, J.L.; Wu, N.C.; Zhu, X.; Kitamura, S.; Wilson, I.A.; Wolan, D.W. An Influenza A Hemagglutinin Small-Molecule Fusion Inhibitor Identified by a New High-Throughput Fluorescence Polarization Screen. *Proc. Natl. Acad. Sci. USA* **2020**, *117*, 18431–18438. [CrossRef]
38. Yang, H.; Carney, P.; Stevens, J. Structure and Receptor Binding Properties of a Pandemic H1N1 Virus Hemagglutinin. *PLoS Curr.* **2010**, *2*, RRN1152. [CrossRef]